TRIBHUVAN UNIVERSITY

INSTITUTE OF ENGINEERING

PULCHOWK CAMPUS

B-06-BAS-2019/24

Design, Fabrication, and Experimental Analysis of Tiltrotor Mechanism

by

Kshitij Luitel (076BAS017)

Kushal Sharma Koirala (076BAS019)

Monika Gurung (076BAS020)

Ujjwal Dahal (076BAS047)

A FINAL REPORT

SUBMITTED TO THE DEPARTMENT OF MECHANICAL AND AEROSPACE ENGINEERING IN PARTIAL FULFILLMENT OF THE REQUIREMENTS FOR THE DEGREE OF BACHELOR OF AEROSPACE ENGINEERING

DEPARTMENT OF MECHANICAL AND AEROSPACE ENGINEERING

LALITPUR, NEPAL

MARCH 2024

COPYRIGHT

TRIBHUVAN UNIVERSITY

INSTITUTE OF ENGINEERING,

PULCHOWK CAMPUS

DEPARTMENT OF MECHANICAL AND AEROSPACE ENGINEERING

The undersigned certify the final year thesis on " DESIGN, FABRICATION, AND EXPERIMENTAL ANALYSIS OF TILT-ROTOR MECHANISM" by Kshitij Luitel, Kushal Sharma Koirala, Monika Gurung, and Ujjwal Dahal has been read and is recommended to the Institute of Engineering for acceptance in partial fulfillment of the requirements for the degree of Bachelor's in Aerospace Engineering.

Supervisor,

Asst. Professor Ashish Karki

DMAE, IOE Pulchowk Campus

External Examiner,

Lecturer Biman Rimal

IOE Thapathali Campus

Tribhuvan University
Institute of Engineering
Department of Mechanical and Aerospace Engg.
Pulchowk Campus

Head of Department,

Asst. Prof. Sudip Bhattrai, PhD

DMAE, IOE Pulchowk Campus

Date: March-12, 2024

ABSTRACT

This paper presents the design and synthesis of a tilt-rotor mechanism for a hybrid UAV that can perform vertical takeoff and landing (VTOL) and fixed-wing flight. The tilt-rotor mechanism allows the orientation of the propulsion system to change from vertical to horizontal or vice versa, enabling the UAV to fly like a helicopter or an airplane. The paper describes the design, mathematical modeling, structural analysis, and fabrication of the mechanism, as well as the design and testing of a test bench and a control system. The paper also evaluates the performance of the mechanism and the system on a bi-copter UAV model and discusses the challenges, limitations, and future enhancements of the project. The paper concludes that the tilt-rotor mechanism is a promising solution for hybrid UAVs that can combine the advantages of both rotorcraft and fixed-wing UAVs.

Key words: *Tilt-rotor mechanism, Bi-copter, Fixed wing*

ACKNOWLEDGEMENT

The project is prepared in partial fulfillment of the requirement for a Bachelor's degree in Aerospace Engineering. First and foremost, we would like to express our sincere gratitude towards our supervisor Asst. Prof. **Ashish Karki** for his constant guidance, inspiring lectures, and precious encouragement without his invaluable suggestions and reviews, it would have been a difficult journey for us.

We would also like to present our sincere respect and thanks to valuable feedback for Head of Department Asst. Prof. **Sudip Bhattarai (Ph.D.)**, Deputy Head of Department Asst. Prof. **Kamal Darlami**, Asst. Prof. **Sanjay Neupane**, and Asst. Prof. **Arun Bikram Thapa** with which we guided ourselves.

We would also like to present gratitude to Research Engineer Mr. **Nabin Bhandari** and Mr. **Sandip Kumar Chaudhary** for their guidance throughout the project and supporting for taking helpful steps in the project. We would also like to present our sincere respect and thanks to Robotics Club, Wood Workshop of IOE Pulchowk Campus, and IIEC for providing us with instruments, machines, and their valuable support throughout the project.

We would like to thank the Department of Mechanical and Aerospace Engineering, Institute of Engineering, Pulchowk Campus for providing us with the opportunity of a collaborative undertaking which has helped us to implement the knowledge gained over these years as a major project for the fourth year, and develop a project of our own that has greatly enhanced our knowledge and provided us with a new experience of teamwork,

We would also like to thank all our friends and families who have directly and indirectly helped us in doing this project. Any kind of suggestion or criticism will be highly appreciated and acknowledged.

Kshitij Luitel (076BAS017)

Kushal Sharma Koirala (076BAS019)

Monika Gurung (076BAS020)

Ujjwal Dahal (076BAS047)

TABLE OF CONTENTS

LIST OF FIGURES

LIST OF TABLES

ABBREVIATION

ANN: Artificial Neural Network

CAD: Computer-Aided Design

CPAC: Conventional Position-Attitude Control

DAC: Disturbance-Commodating Control

DC: Direct Current

DTVC: Direct Thrust Vectoring Control

ESC: Electronic Stability Control

PID: Proportional-Integral-Derivative

PLA: Polylactic Acid

UAV: Unmanned Aerial Vehicle

VTOL: Vertical Takeoff and Landing

CHAPTER 1: INTRODUCTION

1.1 Background

With the development of the aviation industry, the risk factors and usability of the military also increased. During initial developmental phases, aircraft were used for military purposes during World War I and World War II. Despite the end of the world war and physical attacks, the cold war and rivalry remained among the allies and countries that caused the development of aircraft fast enough for surveillance that rivals could not detect. But with the growing technology and the advancement of the weaponry industry, aircraft were at high risk of being put down during hidden surveillance missions on enemy territory. This led to the development of unmanned aerial vehicles capable of performing certain missions as required.

With the development of technology and global reach to the materials and design of aircraft and UAVs, the public got their hand on UAVs to perform general and recreational tasks along with a few vital jobs with risks. This led to the advanced development of rotorcraft and fixed-wing UAVs. Rotorcrafts are UAVs capable of vertical takeoff and landing that have great stability and maneuverability at a lower speed or can stay still in the air when compared to those Fixed-wing UAVs. Whereas fixed-wing UAVs possessed better range, endurance, speed, and aerodynamic performance compared to those rotorcrafts. The diverse property of the two kinds of UAV generalized in the design, the application, and the usability defined the industrial and general usages.

Rotorcraft became popular among the public for photography, drone racing, and recreational activity with short endurance. The development of rotorcraft led to categorization to being coaxial, bi-copter, quadcopter, hex copter, and octa copter. The categorization was based on the number of propulsion units used to drive the rotorcraft, leading to rotorcraft of different shapes and sizes. Further development led to the immense use of Tri copters and other complex geometry rotorcraft. The benefit of such development of rotorcrafts was helpful to industry for applicative purposes as they carried versatility. This industry also focused on increasing horizontal speed, endurance

time, range, and vertical stability. There was always a limitation to its performance because of the geometry and direction of the propulsion system.

Whereas fixed-wing UAVs were popular in industrial applications and mainly used for military purposes. The size of such UAVs ranged from a few grams to hundreds of kilograms as per design. Application in surveillance to drone strikes to the carriage of packages to rural areas, the fixed wing can be designed and used in versatile industries with variable sizes. But such UAVs always required any medium to take off and land during their mission planning. This limited its field of application and zone to operate. Despite having long endurance, range and airspeed, and higher payload fixed-wing aircraft could only be operated through limited space dedicated to launch and recovery.

To overcome the design problem of both types of UAV, the concept and design of hybrid UAV was started which led to the development of UAV that consisted of the pros of both rotorcraft and fixed-wing, i.e., UAVs capable of vertical takeoff and landing and also have an aerodynamic body like that of the fixed wing that can perform long endurance and range mission with less energy consumption and helps to propel the aircraft in the forward direction as that of a propeller in an airplane. The idea led to the design of a propulsion system that can take off any UAV vertically and provide sufficient thrust to move at a vertical distance without stalling. One of the development and project of such aircraft is V22 Osprey which can vertically take off like a helicopter and thus fly like an airplane after gaining the required altitude.

Figure 1.1. 1 V-22 Osprey [1]

Despite the design, production, and development of hybrid UAVs, their use and development are limited only to the research field. This is because of the complexity of

the phase change between the rotorcraft and the fixed wing. The structural loading, propulsion deflection, the balance of moments, torque, and forces were a few of the reasons that hindered the development of the Hybrid UAV. As the industry and application in individual UAV fields are progressing concerning the generation, the need to change to hybrid UAVs is not the primary requirement.

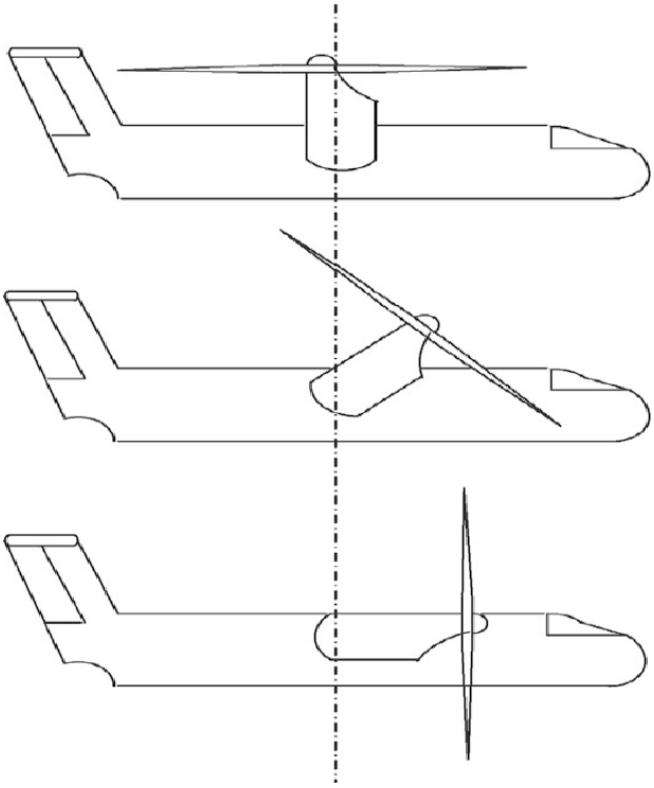

Figure 1.1. 2 Phase of Transition [2]

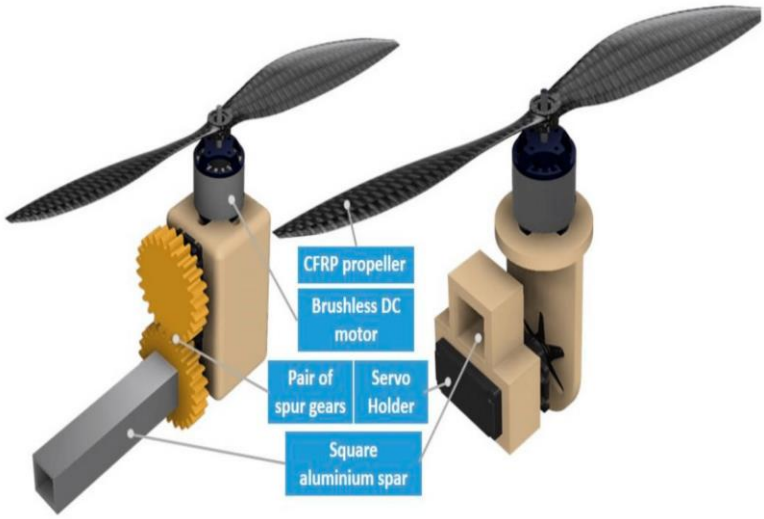

Figure 1.1. 3 Tilt rotor Mechanism [3]

In the scientific field, the design and testing of Tiltrotor aircraft, impressed by V22 Osprey, is on the verge of a breakthrough to hit the general market, but the deep study and analysis of the tiltrotor mechanism are still in its early phase. The tiltrotor mechanism is the mechanical design to transfer the vertical propulsion system to a horizontal or tilted position, as required, during the transition of a hybrid UAV from rotorcraft mode to fixed wing mode. This mechanism can solely be used in rotorcraft to boost up the speed at higher rpm of the propulsion or embed to the fixed wing to reduce its takeoff time. If the mechanism is used in the compiled system of both types of UAV, it gives the versatility of both stability in midair like rotorcraft and horizontal speed, versatile size, and huge payload capacity like of fixed wing, as required. The mechanical design helps with the modification and balancing of UAVs and aircraft in midair along with takeoff and landing time.

1.2 Objective

The main objective of the project is to design, synthesize and experimentally analyze a tilt-rotor mechanism for a hybrid UAV that can perform vertical takeoff and landing (VTOL) and fixed-wing flight. The specific objectives of the project are as follows:

- To design a mechanism that can change the orientation of the propulsion system from vertical to horizontal or vice-versa, enabling the UAV to fly like a helicopter or an airplane.
- To create a mathematical model of the mechanism that can be used for future research and development in the field of UAV design featuring tilt rotors.
- To evaluate the performance of the mechanism in bench test.

The result of this study will be supportive and valuable to pursue the development of tiltrotor mechanisms and setups for aircraft and UAVs. This study will also be valuable to the synthesis of the tiltrotor system for the wing of a hybrid UAV.

1.3 Problem Statement

Existing unmanned aerial vehicles (UAVs) suffer from limitations in terms of their vertical takeoff and landing (VTOL) capabilities, as well as their long-range and endurance flying capabilities. While rotorcraft UAVs, such as quadcopters, excel in

VTOL operations, they are constrained in their ability to cover extensive distances and sustain flight for prolonged periods due to their aerodynamic limitations. Conversely, fixed-wing UAVs offer greater range and endurance but require a runway for takeoff and landing. In certain cases, fixed-wing UAVs are deployed using launch mechanisms and subsequently retrieved upon mission completion. To overcome these drawbacks, tilt-rotor VTOL fixed-wing UAVs have emerged as a viable solution, combining the advantages of both rotorcraft and fixed-wing UAVs. These UAVs exhibit the versatility to perform VTOL operations and fly over long distances for extended durations, making them suitable for a wide array of missions.

1.4 System Requirements

The completion of the project is based on two pillars. Initially, all the design and analysis parts are done computationally, which will benefit in terms of cost, time, and design freedom. Then, the suitable design was fabricated with available materials for bench test.

1.4.1 Hardware Requirements

1. Carbon fiber rod
2. 3D printer and PLA as printing material
3. Propellers
4. Servo-actuators
5. Brushless DC Motor
6. Soldering gun and electronic components such as ESC, Control Board
7. Components for fabrication of Testbench

1.4.2 Software Requirements

1. CAD Modeling- Catia V5
2. Linkage and Mechanism Design and Testing- Linkage
3. Electrical and Electronic Circuit Modeling- Proteus, MATLAB
4. Mathematical Modeling- MATLAB, Python

CHAPTER 2: LITERATURE REVIEW

Tilt-rotor UAV is a hybrid configuration UAV that has the property of vertical take-offs like rotorcraft and flight plan and performance of the fixed wing. The limited capability to overcome the limitation of range and endurance of rotorcraft configuration can be overcome by the usage of Tilt-rotor aircraft. The Nobel design of the tilt-rotor aircraft allows a smooth transition from VTOL to fixed wing overcoming the moments. This type of Hybrid Tilt-rotor mechanism substantially increases the flight range and endurance when compared to the conventional rotorcraft configurations presented [4]. Hybrid UAVs have a widespread application due to flexibility with the environment. From surveillance and aerial footage to payload carry, hybrid UAVs can perform various tasks with necessary adjustments. Hybrid UAVs can overcome the limitations of a fixed-wing UAV like the requirement of takeoff and landing path and UAV takeoff. It also performs significantly better than rotorcraft as the body drag of the hybrid UAV reduces with a tilt of the propellers.

Forward tilting of propellers reduces drag area and thus allows for faster, more agile, and more efficient flight. The mechanism of tilting propellers in quadcopters had 12.5% higher speed and 20% lower power consumption compared to that of quadcopters in the speed range of 15-20m/s. This can have significant applications to time-sensitive and a vehicle frame designed aerodynamically like an airfoil shape to reduce the drag coefficient can significantly boost the performance of the UAV [5].

During vertical takeoff, there are no aerodynamic forces and moments as there is no forward airspeed. The horizontal force produced by tilting the axis of the motor is proportional to the tilt angle and changes gradually from 90 degrees to 0 degrees. Thus, the lift, drag, and moments affect the UAV body, and the transition mode plays a vital role in the stability, movement, and flight mode of the UAV. the transition mode consists of nacelles angle, pitching, and thrust occurring during the phase change of the motor from a vertical position to a horizontal one [3]. However, during takeoff, landing, and hover phases, the wind field has a greater influence on the control stability of the tilt-rotor UAV. Hence, the effect of the gust is significant during these phases. [6]

The comparative performance analysis shows that the tilting takeoff scheme with optimal trajectory showed that it takes 47% less time and 75% less energy than the vertical Takeoff scheme whereas with only a slight difference in energy consumption and time, it can go aerial without any requirement of sliding distance compared to that of short take-off [7].

Tilt-rotor mechanism can be achieved by gear-shifting the mounted motor to the servo for the same specific purpose. However, mathematical modeling is required to validate and apply to the general variable of a similar domain. A direct thrust vectoring control (DTVC) scheme adds the control authority of the rotor tilt mechanism to enable the decoupling of attitude and trajectory and improve the response rate and response bandwidth of the flight trajectory. A robust UAV controller based on the backstepping sliding mode control method determines the stability of the control system through the Lyapunov function. The simulation results show that the DTVC scheme improves landing accuracy and speed compared to the conventional position-attitude control (CPAC) scheme and decouples the position control loop from the attitude control loop, enabling the UAV to complete flight control in the VTOL phase [8].

A UAV can be transitioned from level flight to hovering flight without switching the controller gains and dynamical model. By using the dynamic inversion method in flight control system design, nonlinear equations of motions can be linearized and by employing a robust rotational controller, disturbances like from wind can be mitigated. Disturbance-accommodating control (DAC) method and Kalman filter help to estimate the unknown parameters of the nonlinear equations and the velocity of the UAV. [9] The flight control system for the tiltrotor can be designed using an inner or outer loop control structure and an eigenstructure assignment algorithm based on mathematical modeling [10] [2]. For different control methods, different approaches can be considered as PID for linear control, linear control based on particle swarm optimization method, model inversion technique based on ANN, and active disturbance rejection control. These methods optimize the gain scheduling control, compensate for the model inversion error and ANN adjusts the PID parameter for smooth switch control [9] [2]. There exist few mathematical models [2] that define the control mechanism for the hybrid UAV, but a specific definition of the mechanism is yet to be defined that is universal to the system.

The stability model for the phase change of the system is not smooth enough to be implemented in the system without prior testing. However, there exists the stability criterion for fixed wing UAV and rotorcraft separately, the definitions and exact mathematics for the hybrid UAV are yet to be defined. Thus, mathematical modeling that can define the general stability criteria for the tiltrotor mechanism leads to definitive static stability.

The transition of the phase from rotorcraft to fixed wing UAV can be defined by the different types of mechanism conventionally available [11]. Of the available mechanisms and machines, 4-bar mechanism, connectivity with meshing of gears, using of belts to connect, and coupling of the connecting rods can be effective to work with. However, there exists numerous mechanisms, effective design to tiltrotor can be evaluated by its capability to be used, performance, contribution to drags and aerodynamic forces, and its weight when prototyped. The shifting of the propulsion system also changes the center of gravity of the UAV, thus affecting the calculations of the UAV. Thus, the mechanism used for transition must be effective enough that the major shift of the C.G. does not occur, and calculations of the flight and control are not to be evaluated separately.

The system to be designed may not effectively be stable to the mechanical and aerodynamic forces, thus, the physical testing of the mechanism is to be performed for the thrust generated by the connected motors, performance of mechanism and its effectiveness to the system, fluttering of the connecting rods with reference to the C.G. of the UAV, and ground effect generated by the motor. Furthermore, the transition phase produced by the servo connected to the mechanism has to be analyzed whether it is effective to full flight condition and optimized for performance. The design of the test bed must be effective enough that the data of test be recorded in both horizontal and vertical conditions and even in transition phase. The required data to be recorded for the evaluation of the system is thrust in horizontal and vertical direction and effect of the motor and servomotor to the transition phase, thus, usage of load-cell is effective enough for the testbench.

The availability of the different types of control board has diversified the usage of it. However, because of complexity of the programming, the compiling and usage is

limited. The Arduino boards provide user friendly interface with huge library that consists of numerous codes that are open sourced that helps to calibration and measurement of thrusts [12]. This interface and board support for easy calibration and designing of systems compatible for testbench. It also provides a valuable platform for the initial phase for testing and calibrating motors and servomotors.

The availability and selection of components hugely affect the performance of the mechanism and even the UAV to be modeled [3]. Thus, the selection of major components must be reviewed using the performance charts and manufacturer's provided manuals and results. There are thousands of BLDC and servomotor available, for the objective to be fulfilled, BLDC with high output thrust performance with effective propellers, servomotors with effective torque is to be selected [4] [13].

The initial vision is to develop a stable and capable tiltrotor mechanism for a bi-copter rotorcraft that can transition to fixed wing UAV while hovering and that has capability of takeoff, cruise, and landing. Despite the study and proposing of VTOL capable fixed wing UAV, the UAVs available in pre-programmed UAV flight control and researches are delta wing tri-copter and penta-copter that uses a separate duct fan for horizontal flight and remaining for vertical flight and some with quadcopter that shifts whole wing for the flight plan [5] [3] [7]. Also, the available bi-copter type model clearly does not define the mechanism to be used for the tilting of propulsion system and are based basically on scaled model of V22 Osprey and design of flight control rather [14] [15] [16] [17].

CHAPTER 3: METHODOLOGY

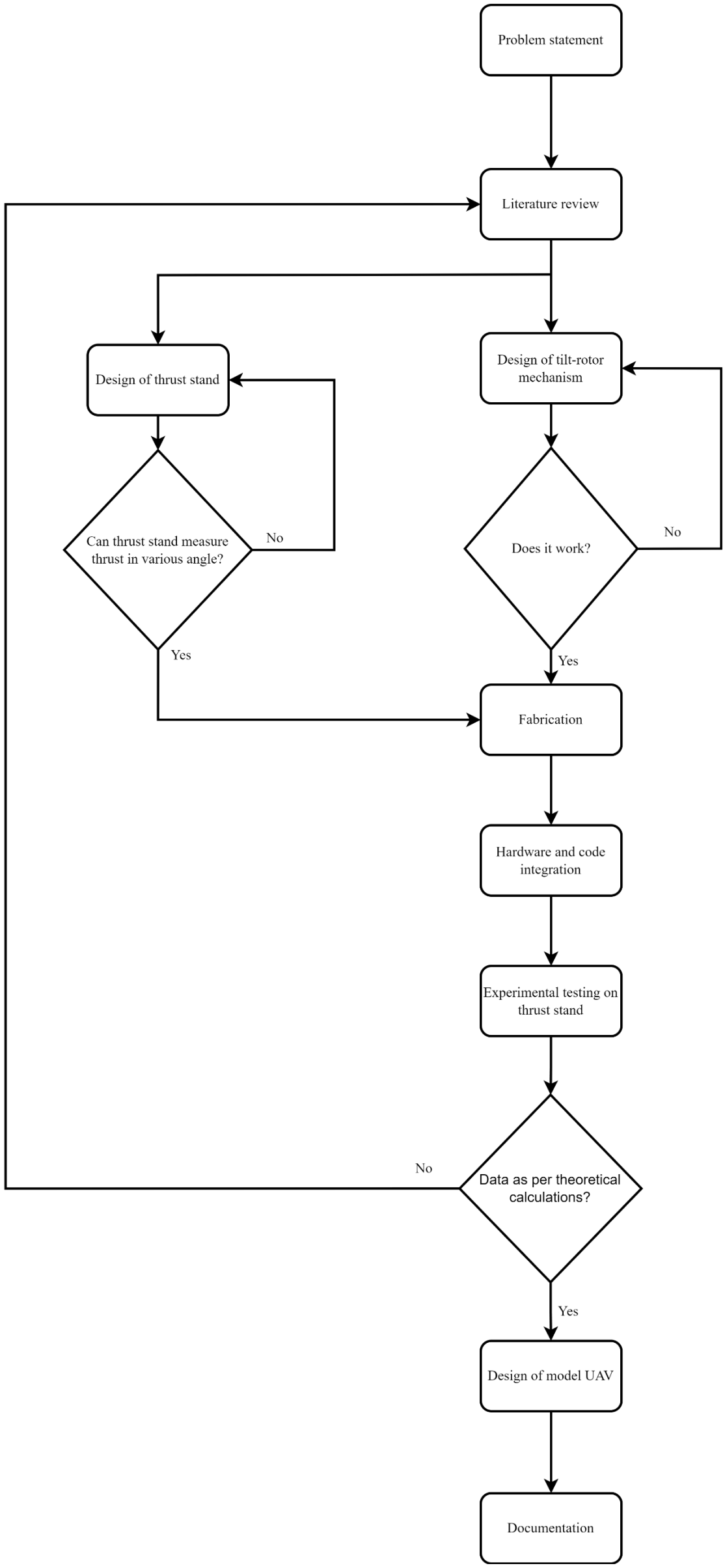

Figure 3. 1 Methodology Chart

The initiating step of the project is a literature review and conceptual design. With the available references, a CAD model of the tilt mechanism is to be designed. The CAD model is analyzed for structural stability and performance analysis with the available model and design. The model will be then fabricated as per the design for testing on the testbench.

Before the testing of the fabricated model in the testbench, the control system/mechanism will be designed specifically for the model and tested if applicable. The testbench is also to be designed simultaneously with other design activities and tested. If the control mechanism is successful, the control circuit will be fabricated and then embedded in the tilt-rotor mechanism.

Then, the fully fabricated model of the tiltrotor mechanism and control system will be tested and analyzed in a testbench for static stability, structural rigidity, and performance for on-flight tests. If the test on the testbench is successful, the system will be tested in a real environment. The successful model of the tiltrotor mechanism will be then assembled onto the bi-copter UAV and tested on a flight for the feasibility of the system for hybrid UAV.

3.1 Phase I

3.1.1 Design of Tilt Rotor Mechanism

A major part of this project is to analyze and select the compatible mechanism for the hybrid UAV that has capability of vertical takeoff and landing and horizontal cruise. The available designs of mechanisms and machines will be reviewed to apply it to the system. With the compatible mechanisms selected, the possible designs and methods to integrate will be considered. Thus, using the knowledge of mechanisms from lectures and books and capability to play with the design, system capable to handle the requirements will be designed. With the initial design, visual analysis and FEM will be done to check the mathematical and engineering compatibility.

If the design is proven to be compatible and capable of handling the requirements, it will be reviewed by manufacturing its prototype and testing it physically for strength. This will be done as the actual properties and capabilities of the materials to be used

are not clearly defined for the environmental conditions. This will help to modify and iterate the design in CAD to optimize the initial designing idea.

3.1.1.1 Bending Within Permissible Range

The designed model will be analyzed through analysis for static condition within CAD software for its bending and disorientation by assigning approximate values of the materials available for 3D printing. This will give a generalized idea of which material to be used and will greatly benefit in the study of the material and mass of the mechanism after printing.

Selection of material will be important as this will specify the limits of the system and the environment that the mechanism and system will function and fail. The selection will be primarily based on two parameters; one of being the references and manuals provided online and by manufacturers, and second being by printing the same part with all the materials available and test under same conditions for failure and performances. This will help to shortlist the materials to be used.

3.1.2 Design and Analysis of Testbench

This phase of the project will focus on designing a compatible testbench that can be used for measuring the required parameter in required ways. As per our project, designing of the testbench and performance of it is vital as major of the analysis of the mechanism and system will be done with the available data from the test bench. Thus, for reliability of the system, the testbench will be analyzed thoroughly through its capability of measuring the forces, thrusts, and masses acting in 2D plane. The designing of testbench will be based on two phases as initially to measure the thrust on the connecting rod and mechanism and visual inspection on fluttering and bending of connecting rod, and secondly to measure the parameters of the UAV to check the compatibility of the mechanism after assembly.

The selection of hardware and sensors to calibrate and measure the required parameters will also be done by comparison of the available hardware and sensors and secondary parts to be designed to embed to system for measurement. The test bed will be designed such that it will be rigid and not be affected easily by the drag and forces exerted by the

system. It will also be ensured that the testbench will be versatile for modification for further use and be capable of measuring the required parameters as designed to do.

Selection of material for designing the testbench will also be performed as the durability, reliability, and rigidity of the testbench will hugely impact the design and analysis of the project and the mechanism. The test bench will be assembled and calibrated for precision reading and accurately measure the parameters as required.

3.1.3 Design of Control System for Preliminary Phase

In initial phase, the project will be focused on designing of tiltrotor mechanism and assembly of it to the connecting rod, designing of the testbench, fabrication of designs and their assembly and initial calibration and preliminary testing of the system as required. Then there will be a requirement of control system for all of these. The control system will be programmed as per the available and required boards for the system assembly (mechanism and testbench). As per the requirements, control of servomotors, BLDC, and hardware and sensors will be programmed and run through for calibration and testing of the software. As per the available board for the phase, programming may vary, and alternatives will also be looked upon.

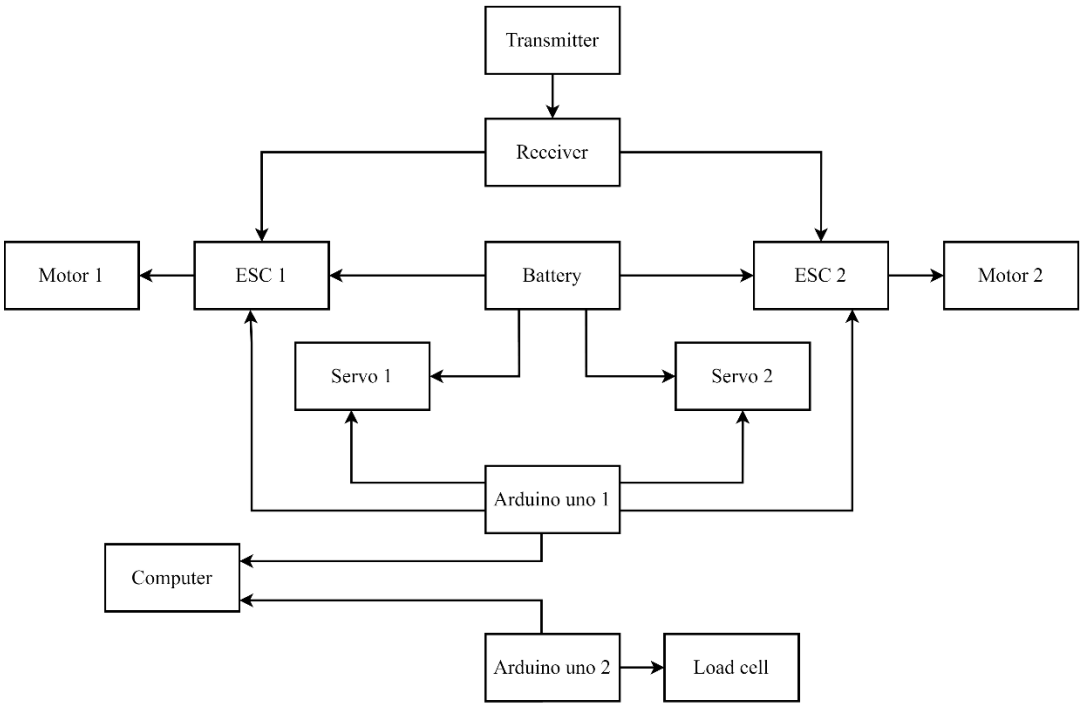

Figure 3.1.3.1: Block diagram of control system for bench test

3.1.4 Fabrication

After the succession of design and computer-based analysis of mechanism and the testbench, the parts of the mechanism and the testbench will be fabricated for testing on testbench. As per the selected materials, all the parts, hardware, and sensors will be fabricated and assembled for measurement of parameters as required. In case of failure of fabricated parts and mechanism, the CAD design will be re-evaluated and modified as requirements and refabricated until satisfied.

Not only for the mechanism, the fabrication of testbench will also be watched over as requirements and modified, redesigned, and refabricated with each failure and modifications requirements. This will ensure that the design and mechanism will successfully perform in the real environment too.

3.2 Phase II

3.2.1 Initial Testbench Assembly

In phase 2, the fabricated mechanism will be assembled to the connecting rod and further to testbench after all the required electronics are connected to the system. In this phase initially, the desired assembly of the electronics (BLDC, servomotor) to the mechanism and electronic connection of these to the control board and programming them will be done. Simultaneously, the hardware and sensors will be assembled to the testbench and then to an electronic control board. Then, balancing the system, the connecting rod with the mechanism assembled will be inserted and assembled to the testbench for further study.

3.2.2 Data Collection

After assembly of the system and running it, data will be collected as requirement for different variables with multiple testing for accuracy and precision. The data will be collected and recorded through the control boards. Along with data collection and testing of the transition of the propulsion system, the visual inspection of the connecting rod will be performed for fluttering and bending because of the thrust, and forces acting on it.

The collected data will be plotted as required for analyzing the thrust produced in different phases of transition in different variables (variable rpm, variable transition time or both). The plotting will be studied for optimizing the parameters that can be played with and design the optimum UAV as per the mechanism designed. The data and plotting will also be used to modify the existing design of the mechanism.

3.3 Phase III

Phase 3 is the supplementary phase of the project that will only be done with the availability of the time and materials. The initial phase 3 consists of designing of UAV and prototyping it, which will be done with the successful test of the mechanism.

3.3.1 Design of UAV

As per the performance of the mechanism in testbench, UAV will be designed to compatibility of vertical takeoff and landing and horizontal cruise and mission. During the design of the UAV, selection of airfoil, control surfaces, and analysis of the UAV will be performed using available software by varying change in C.G. As the mass of the UAV is to be limited, the designing phase will be constricted to play with limited variable during design. As for the calculation and primary analysis of the mechanism, a novel UAV is required which is statically and dynamically and be fabricated if required. Thus, with an initial mass estimation of 2 kg of UAV, a UAV was designed of properties as mentioned.

After the analysis, an approximated UAV is designed.

Table 3.3.1 1 Conceptually Approximated UAV Parameters.

PARAMETERS	SPECIFICATION
UAV	VTOL, Tiltrotor
Wingspan	124 cm
Wing Cord Length	22 cm
Wing Area	0.267 m^2
Wing Airfoil	Sd7062
Position of C.G. in X axis	6 cm from L.E.
Lift coefficient at 0^0 AOA	0.445

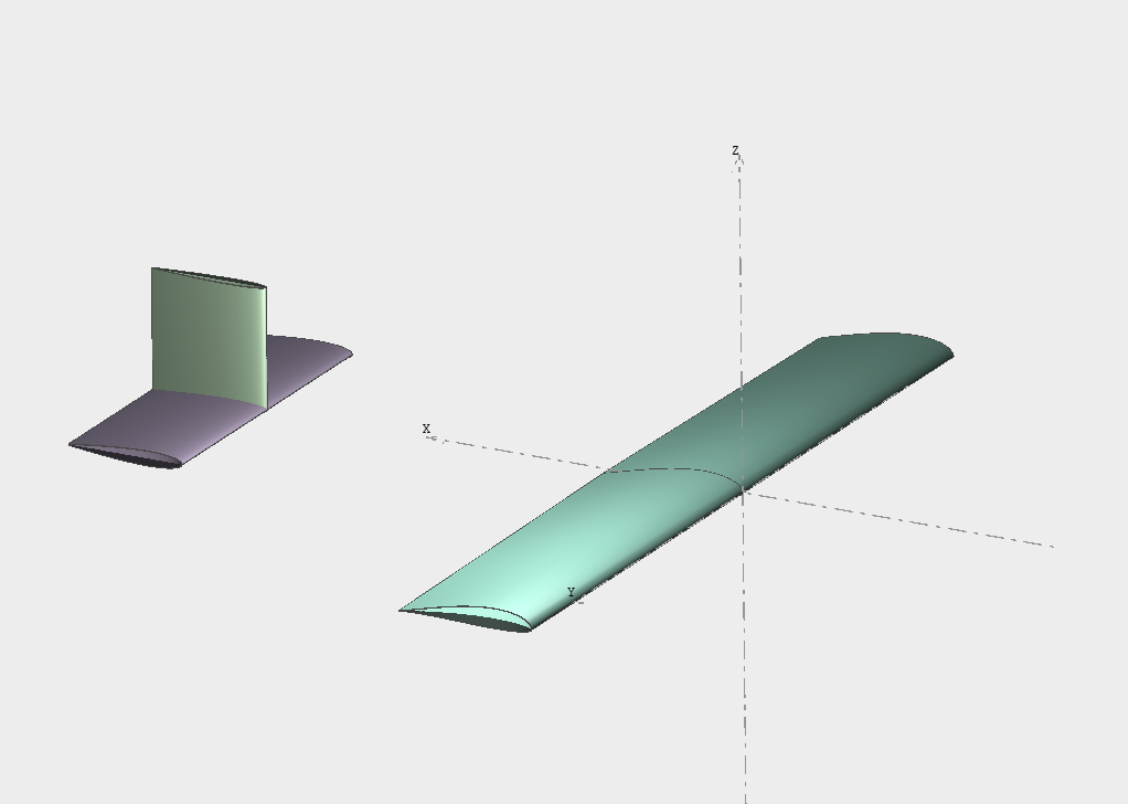

Figure 3.3.1. 1 Schematic Diagram of UAV Designed.

3.3.2 Selection of Flight Control Board

Out of the available flight control boards, only a few of the boards provide open source bi-copter VTOL control command (program). The flight control board and command will be selected out of the available ones and those compatible to the project (UAV).

3.3.3 Bench Test

The designed UAV will be taken to testbench/testbench for bench test for data collection and the output data and plotting will be used for optimizing the UAV. The plotting from the data collected will be used to assume for the real environment and optimize the UAV for its first test real-environment flight.

3.3.4 The Flight

After the completion of the designing of the UAV, selection and modification of control boards and program, and bench test for stability and capability of flight, the flight of the UAV will be done.

CHAPTER 4: RESULT AND DISCUSSION

4.1 Mathematical Modeling

The purpose of the project was to create a suitable and applicable tiltrotor mechanism for VTOL UAV. Thus, the functioning and control of both conditions, i.e., rotorcraft and fixed wing UAV had been considered. This laid the pathway to creating a hybrid mathematical model to consider all the properties of both types of UAV.

The transition state is the phase transition in between them, where properties from both types play the role in force, moment, accelerations, and velocities along with the UAV's stability.

Initially, considering the kinematics of bicopter, the UAV must be analyzed by two frames of references i.e.,

- Earth fixed frame of reference (X_E, Y_E, Z_E)
- Body fixed frame of reference (X_B, Y_B, Z_B)

The position and attitude of the center of mass of the UAV with reference to earth fixed frame of reference be defined as

$$n_1 = \begin{bmatrix} x \\ y \\ z \end{bmatrix}$$

$$n_2 = \begin{bmatrix} \emptyset \\ \theta \\ \psi \end{bmatrix}$$

Here, x, y, z represents the position of the UAV and Φ, Θ, ψ represents the Yaw, Pitch, Roll of the UAV representing center of mass of the UAV by Euler's angle representation.

The complete pose of the UAV in Earth fixed frame of reference using Euler's orientation is given as

$$n_E = \begin{bmatrix} n_1 \\ n_2 \end{bmatrix}$$

The change of position of the UAV in Earth fixed frame of reference with respect to center of gravity gives the velocity of the UAV in Earth fixed frame of reference, i.e.

$$n'_E = \begin{bmatrix} n'_1 \\ n'_2 \end{bmatrix}$$

Here, n'_E *represents* Euler's overall velocity, n'_1 represents the linear velocity and n'_2 represents the angular velocity in the Earth fixed frame of reference.

As, the velocity of the UAV recorded within the UAV is based on the Body fixed frame of reference of the UAV with the sensors attached within the UAV, the velocity can be represented as

$$V_1 = \begin{bmatrix} V_x \\ V_y \\ V_z \end{bmatrix}$$

$$V_2 = \begin{bmatrix} p \\ q \\ r \end{bmatrix}$$

Here, V_x, V_y, and V_z represent linear velocities in three respective axis and p, q, r are the angular velocities in X, Y, Z axes respectively in Body fixed frame of reference, which are given by the sensors calibrated and attached to UAV.

$$V_B = \begin{bmatrix} V_1 \\ V_2 \end{bmatrix}$$

Kinematically, the relationship between the Earth fixed frame of reference and the Body fixed frame of reference be defined in terms of velocity relation as

$$n'_E = J \times V_B$$

Where, J is the Jacobian matrix, which is dependent and function of yaw, pitch and roll on the UAV.

$$J = \begin{bmatrix} J_1 & 0_{3*3} \\ 0_{3*3} & J_2 \end{bmatrix}$$

where, J_1 is the transformation matrix for linear parameters and J_2 is the transformation matrix for angular parameters.

Dynamic modeling of the UAV is necessity to address the aerodynamic lift and drag forces produced by the wing and vertical thrusts from the propulsion system. These properties are incorporated for transition phase, resulting in mixed horizontal and vertical dynamics.

For consideration of dynamic mathematics, entire UAV is considered rigid, earth's rotation is considered negligible in comparison to Body fixed axis acceleration, X-Z axis of body axis is considered as plane of symmetry, and relative change of position of mass to C.G. even when the propulsion system is tilted from vertical to horizontal position or vice-versa.

The dynamic equations for body-fixed frame of reference with Euler's formulation can be expressed as:

$$F_1 = mV'_B + \omega_B \times (mV_B)$$

$$M_1 = I\omega'_B + \omega_B \times (I\omega_B)$$

Here, F_1 is the total external force exerted in the body and M_1 is the total moment acting on the C.G. of the UAV. V'_B and ω'_B are the linear and angular accelerations of the UAV in the body fixed axis respectively. *I* is the inertia of the UAV.

The total external force acting on the body can be expressed as,

$$F_1 = F_{prop} + F_g + L_w + D_w + F_{gust}$$

where,

$F_{prop} = \begin{bmatrix} F_R sin\xi_R + F_L sin\xi_L \\ 0 \\ F_R cos\xi_R + F_L cos\xi_L \end{bmatrix}$ is the thrust exerted by the propellers; ξ is the angle of tilt of rotor from vertical position to horizontal position, and F_R and F_L are the thrust from right and left rotors respectively.

$F_g = \begin{bmatrix} mgsin\theta \\ -mgsin\emptyset.cos\theta \\ -mgcos\emptyset.cos\theta \end{bmatrix}$ is the force due to gravity.

$L_w = \begin{bmatrix} 0 \\ 0 \\ qsC_l \end{bmatrix}$ is the lift generated by the wing.

$D_w = \begin{bmatrix} -qsC_d \\ 0 \\ 0 \end{bmatrix}$ is the drag of the UAV; q is the dynamic pressure.

F_{gust} is the external unknown gust and forces that act on the C.G. of the UAV. [3]

The dynamic equation for the overall moment acting in the C.G. position of the UAV is:

$$M_1 = M_{prop} + M_{gyro} + M_{aero} + M_{con}$$

where,

$M_{prop} = (lxF_R) + (lxF_L)$; is the moment generated by the propulsion system attached and l is the position of the propulsion system.

M_{gyro} is the gyroscopic moment generated in the UAV.

M_{aero} is the moment generated due to the aerodynamic forces Lift and Drag.

M_{con} is the moment due to control surfaces.

The main goal of this Project is to design the tiltrotor mechanism for novel VTOL hybrid UAV.

The considerations for the tilting Mechanism are as follows:

- During the rotation of the propulsion system from Vertical to Horizontal position, the C.G. position of the UAV in XZ plane remains unchanged.
- The UAV is hovering with no vertical, horizontal, or directional velocity, just prior to the tilting starts.
- There exists no external moments and gust force during the transition.
- Velocity at horizontal condition is known and is equal to $1.2 \times V_{stall}$ of the UAV.
- Angle of Attack of the UAV is 0 for every instance of the transition.

Considering only the thrust is provided through the propulsion system, and the UAV is at 0 velocity in each direction, the required Lift to hover and not loose altitude at each angle is approximated along with the available force at each instance in X direction to accelerate.

With the required lift plot for each angle, using the mathematical equation for Lift, approximated velocity at each angle to generate the lift is calculated and velocity plot is generated.

However, because of the velocity, drag is generated that reduces the available force for acceleration in X direction. Interpolating all the forces involved, acceleration available and velocity required is determined. This generates the required time for autonomous transition of the propulsion system as desired.

Initially, calculations for lift are performed with the condition that the thrust generated through the propulsion system is equal to the weight of the UAV. i.e.,

$$F_{Rotors} = W \times g$$

With the above assumptions, value of F_{1z} at each instance is determined by using the dynamic model of the UAV. Also, F_{1x} is noted as initial approximated available thrust. As the tilt of the rotors cannot sustain the weight of the UAV, the F_{1z} gives negative readings for each value of the tilt angle, which is the amount of Lift required to hover as initial condition.

$$\therefore L_{req} = (-1) \times F_{1z}$$

With the above guiding equation, velocity for each instance is calculated through the Lift equation. i.e.

$$L_{req} = \frac{q \times s \times C_l \times V^2}{2}$$

$$\therefore \frac{q \times s \times C_l \times V^2}{2} = (-1) \times F_{1z}$$

$$\therefore V = \sqrt{\frac{-2 \times F_{1z}}{q \times s \times C_l}}$$

Thus, the equation for the velocity provides the minimum required velocity to hover at that initial condition. However, with the velocity, drag force is exerted in the UAV that acts on the X direction of the flight.

$$D_{gen} = \frac{q \times s \times C_d \times V^2}{2}$$

The drag equation shows that with velocity increase in each instance of the flight, the drag force acting on the UAV increases.

The effective force at each instance in tilting in X direction that produces acceleration is given as

$$F_{x_{eff}} = F_{1x} - D_{gen}$$

The effective force is the net force that acts on the UAV to generate acceleration and drive the UAV forward.

$$\text{i.e.} F_{xeff} = m \times a_{gen}$$

where, a_{gen} is the acceleration generated in between two instances.

$$\therefore a_{gen} = \frac{F_{xeff}}{m}$$

$$a_{gen} = \frac{F_{1x} - D_{gen}}{m}$$

As the drag of the system changes continuously, the effective acceleration varies continuously, thus, it is better to discretize the transition into small intervals and velocity for each discretized point(angle) can be calculated and drag generated at that point and thus, the effective force.

As we know, a_{gen} is the acceleration available that transits velocity in between two consecutive discretized points, it can be expressed as,

$$a_{gen} = \frac{V_i - V_{i-1}}{t}$$

where, V_i is the velocity required at that discretized point and V_{i-1} is the required velocity at previous discretized point and t is the required time to transit between *i-1* to *i* point.

$$\therefore t = \frac{V_i - V_{i-1}}{a_{gen}}$$

For actual transition consideration, there can be different aspects to transit and reach from vertical position of propulsion system to horizontal position. However, few of them can be taken as effective to conserve the properties of altitude and attitude.

Approach 1: Variable ω Approach

In this approach, the time required to tilt is initially fixed, and transition from vertical to horizontal is linear, i.e., each interval of time, equal Θ angle is tilted.

However, in the initial condition (Θ= 0), lift is sufficient to hover, the z-component decreases with respect to change in Θ, thus, to keep the Z-component of thrust constant to uplift at same height, RPM of motor must be increased with respect to change in angle of tilt.

i.e. for each angle Θ_i, thrust through motor must be,

$T_{\theta i} = \frac{T_0}{\cos(\theta_i)}$, where T_0 is the thrust @ 0^0 or vertical condition & Θ_i angle of tilt of rotors.

We know, $T=k\times\omega^2$

$\therefore \omega_{\theta i}{}^2 = \frac{\omega_0{}^2}{\cos(\theta_i)}$ Here, $\omega_{\Theta i}$ is the required angular velocity of propellers at each Θ instance.

As change of thrust is dependent to sinusoidal curve, linearizing it into intervals to find the slope and sensibly making calculations easier,

Taking interval of 15^0 each thus, each 15^0 is covered in $\frac{t}{6}$ sec.

Table 4.1. 1 Representation of Angle, Thrust, RPM, and Slope

Angle	Thrust	ω	Slope
0	T_0	ω_0	0
15^0	T_{15}	ω_{15}	Slope (0-15)
30^0	T_{30}	ω_{30}	Slope (15-30)
45^0	T_{45}	ω_{45}	Slope (30-45)
50^0	T_{50}	ω_{50}	Slope (45-50)

During transition, @45^0, V_{stall} is reached with that assumption and calculations, it is calculated that lift through wing is effective. The range of 45^0 to 50^0 is kept such that margin of safety is provided during calculations.

From calculations,

Table 4.1. 2 Table Relating Thrust at Specific Angle with Respect to Previous Angles.

$T_{15} = 1.035 \times T_0$	
$T_{30} = 1.155 \times T_0$	$T_{30} = 1.115 \times T_{15}$
$T_{45} = 1.414 \times T_0$	$T_{45} = 1.035 \times T_{30}$
$T_{50} = 1.5556 \times T_0$	$T_{50} = 1.10 \times T_{45}$

Table 4.1. 3 Table Relating RPM at Specific Angle with Respect to Previous Angles.

$\Omega_{15} = 1.017 \times \omega_0$	
$\omega_{30} = 1.0747 \times \omega_0$	$\omega_{30} = 1.0559 \times \omega_{15}$
$\omega_{45} = 1.189 \times \omega_0$	$\omega_{45} = 1.1068 \times \omega_{30}$
$\Omega_{50} = 1.249 \times \omega_0$	$\omega_{50} = 1.05 \times \omega_{45}$

Effectively from 0-15, rate of increase of ω per Θ angle is 0.11% of ω_0, from 15-30 is 0.37% of ω_{15}, and from 30-45 is 0.712% of ω_{30}.

i.e., in each $\frac{t}{90}$ sec, 0.11% of ω_0 should be increased from 0 to 15, 0.37% of ω_{15} should ∴be increased from 15 to 30 and 0.712% of ω_{30} should be increased from 30 to 45.

Now, from 45^0 to 90^0, thrust available to accelerate at 45^0 is $T_{45} \times \sin(45^0)$ which is $1.41 \times T_0$.

Now, $1.41 \times T_0$ is used to accelerate UAV of mass m.

$\therefore 1.41 \times T_0 \times \sin(45^0) = m \times a_{45}$

$\therefore a_{45} = \frac{1.41 \times T_0 \times \sin(45)}{m}$

Approach 2: Variable Time Approach (Altitude Decay Approach)

Initially, from available mathematics, required transition time is approximated for intervals. However, the lift is provided by wing even below V_{stall} in calculation, because of boundary layer separation and evidently no valid experiment to prove the existence of lift in our project, it is considered ineffective.

∴ The UAV decays its altitude. Efficiently, decay of altitude can be prevented by increasing the rotation of the motor, however, as it is kept constant throughout the transition. Decayed altitude can be calculated as follows.

Let the consideration be V_{stall} is reached in 45^0 tilt angles. Let the consideration be the altitude decays up to 50^0 to consider the calculation.

Table 4.1. 4 Table Representing Insufficient Thrust at Specific Angles and Acceleration Produced.

Angle	Vertical Thrust through Propellers	Insufficient Thrust as angle tilts wrt. thrust at 0^0 tilt angle	Acceleration due to the thrust in Vertical Axis
0	T	-	0
10	0.985×T	0.015×T	$\frac{0.015 \times T}{m}$
20	0.9397×T	0.0603×T	$\frac{0.0603 \times T}{m}$
30	0.866×T	0.134×T	$\frac{0.134 \times T}{m}$
40	0.766×T	0.234×T	$\frac{0.234 \times T}{m}$
50	0.643×T	0.357×T	$\frac{0.357 \times T}{m}$

The transition time is basically short and as response from servomotor cannot be varied in such short period, total transition is discretized into three intervals of $0\text{-}30^0$, $30^0\text{-}60^0$, and $60^0\text{-}90^0$. Let the time be t_1, t_2, and t_3 respectively. Thus, generalizing velocity and altitude decay, we get,

Table 4.1. 5 Table Representing Acceleration, Velocity Gained, and Altitude Decayed due to Insufficient Thrust due to Tilting of Propulsion Platform.

Angle	Acceleration (a_i)	Time (t_i)	Velocity(v_i)	Altitude Decay $x_i = x_{i-1} + v_{i-1} \times t_i + \frac{a_i \times t^2}{2}$
0	0	0	0	0
10	$\frac{0.015 \times T}{m}$	$t_1/3$	$v_1 = v_0 + a_1 \times t_1$	$x_1 = x_0 + v_0 \times t_1 + \frac{a_1 \times {t_1}^2}{2}$
20	$\frac{0.0603 \times T}{m}$	$t_1/3$	$v_2 = v_1 + a_2 \times t_2$	$x_2 = x_1 + v_1 \times t_2 + \frac{a_2 \times {t_2}^2}{2}$
30	$\frac{0.134 \times T}{m}$	$t_1/3$	$v_3 = v_2 + a_3 \times t_3$	$x_3 = x_2 + v_2 \times t_3 + \frac{a_3 \times {t_3}^2}{2}$
40	$\frac{0.234 \times T}{m}$	$t_2/3$	$v_4 = v_3 + a_4 \times t_4$	$x_4 = x_3 + v_3 \times t_4 + \frac{a_3 \times 4^2}{2}$
50	$\frac{0.357 \times T}{m}$	$t_2/3$	$v_5 = v_4 + a_5 \times t_5$	$x_5 = x_4 + v_4 \times t_4 + \frac{a_5 \times {t_5}^2}{2}$

4.2 Outcome

The outcome of the project can be listed in multiple subheadings explaining the design iteration process, numerical presentation of the mathematical model of the transition, and experimental results.

4.2.1 Design of Mechanism and Servo-Motor Hub

With the study of different types of mechanisms and their properties, four types of mechanisms fitted out requirement. The initial requirements of the mechanism were as follows:

- Rotate BLDC motor from vertical to horizontal position and vice versa.
- Capable to be fitted to small system.

- No mechanical complexity in both design and fabrication.

The mechanisms are:

1. 4 bar mechanism
2. Connecting the rotating platform to servo through belt
3. Gear meshing.
4. Coupling the platform and the servo

4.2.1 4 Bar Mechanism

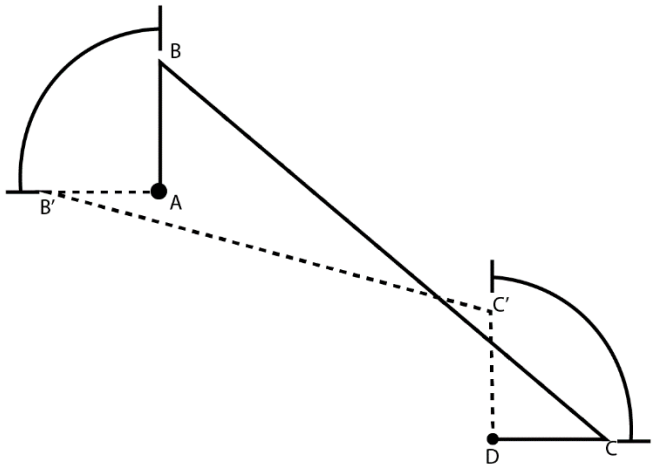

Figure 4.2. 1 Schematic Diagram of Four Bar Mechanism

In the 4-bar mechanism, servo is connected to A-B rod keeping A fixed and B with capability to rotate through 90^0. The length of A-B and C-D are equal such that the angular displacement of both arm is equal. In this mechanism, the base of the BLDC motor is fixed to D such that it can only rotate through it. From C-C'.

Despite having simpler design and theoretical capability to perform in tilting the propulsion system as required, the design is rejected for the following reasons:

a. It cannot be specified that the motor will rotate form C-C' but not go further counterclockwise of C', jamming the mechanism to perform in backward.

b. The design and fabrication of arm B-C plays a vital role as if it is made of lighter material that easily bents, the rotating of servo may not transfer the torque and thrust to the rotation of the motor, and if made of rigid material, the system will be heavy such that it impacts hugely in design of UAV.
c. The system will be bulkier and must be placed beyond the trailing edge of wing requiring extra support that adds dead weight to the system. Also, if placing over the wing changing the direction, it hinders the wings' aerodynamic properties.
d. The assembly of the mechanism will increase the drag to the UAV.
e. Whether changing the arm length ratio of A-B and C-D, the above-mentioned problems cannot be overcome as the limitation of available high torque servo for rotation is 176^0.

Despite having few of the pros, the mechanism was rejected in initial design phase within linkage diagram design.

4.2.2 Connecting the Rotating Platform to Servo Through Belt.

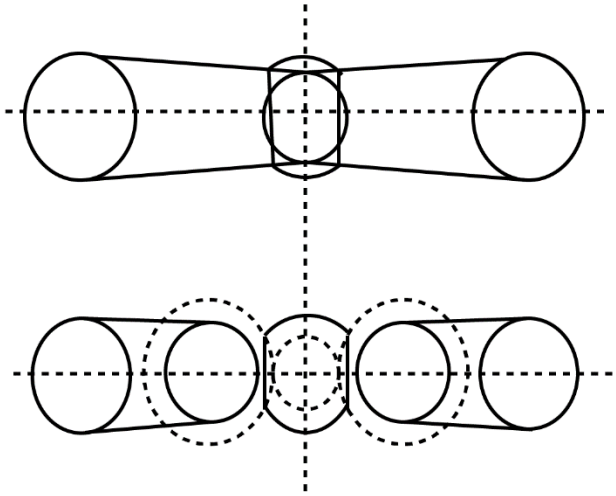

Figure 4.2. 2 Schematic Representation of Belt System Mechanism

Belt connecting mechanism is one of the unique methods to transfer torque from a position. In this method, only one servo is placed centrally/ aligning the propulsion system that will rotate the platform in which the propulsion system (BLDC motor) is mounted. However, the direction of servo rotation and the platform to be rotated does not match, thus, bevel gear is used to transfer the torque through 90^0 rotations.

This system was rejected for the following reasons:

a. If the belts are connected using only the servo, the position of two BLDC motors will not align, thus generating moment and affecting the C.G. position.
b. If alternatively, two gears are used to connect through the servo, the system turns to a bulk.
c. The reliability of belt in the given mechanism and assembly within the wing of the UAV is very vast and difficult to perform.
d. Usage of bevel gear increases the dead weight of the mechanism and increases designing complexity.

Ultimately, without consideration to move forward with the design, the mechanism was rejected. The system is unique and can perform only with one servo placing centrally, but the accessories and complexity made it harder to consider moving forward with the design.

4.2.3 Gear Meshing

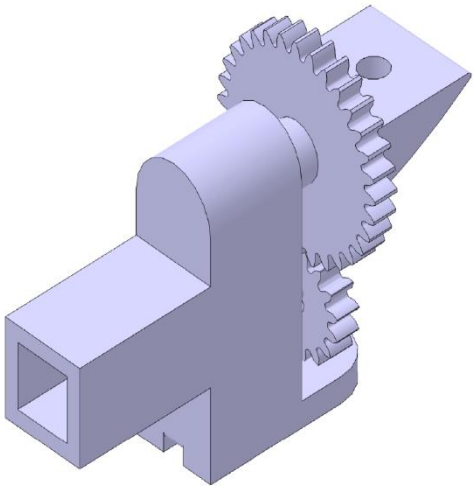

Figure 4.2. 3 Initial Version of Gear Mesh Mechanism

One of the best methods to transfer torque and rotate the platform for tilting the propulsion system is using gear meshing. In this mechanism, two gears with the same module are meshed. The gear ratios can be changed as per requirements too. One of the gears is connected to the servomotor and in the other gear, propulsion platform is connected and rotated accordingly.

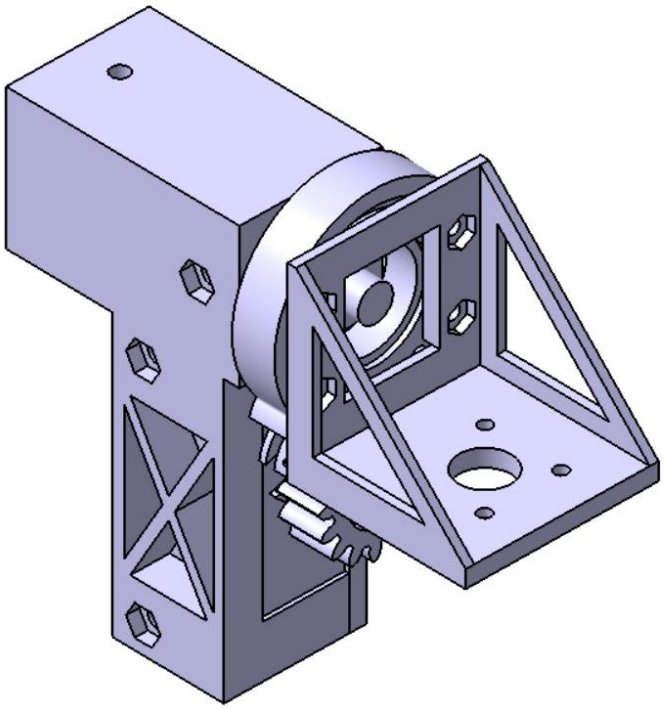

Figure 4.2. 4 Iterated Design of Gear Mesh Mechanism

The benefits of considering the gear meshing system are:

a. The system is reliable, and functions as required.
b. The gear ratio can be changed to vary the time variance for tilting of the propulsion system from vertical to horizontal or vice-versa.
c. The fabrication of the system is easy.

The mechanism was considered and designed, and computer-aided analysis was performed, in which it performed as requirements. Thus, the design was fabricated for further testing and physical analysis. The mathematical calculation for the system is based on gear ratio:

(Servo Gear/Motor Gear) = 1:2

Thus, for every 180^0 rotation of Servo, Motor rotated through 90^0. This was done so that there is an increase of torque.

Thus, with this principle, the initial model was fabricated by 3D printed PLA material. The printed mechanism failed because the gear teeth in contact deformed when loaded (weight of propulsion system). To overcome this problem, ABS material was used for

printing. This provided mechanical superiority and made the printed mechanism more reliable. The comparison of the available materials used for printing is:

Table 4.2. 1 Comparison of Properties of Different Type of Printing Material.

PROPERTIES	ABS	PLA
Tensile Strength	27 MPa	37MPa
Elongation	3.50%	6%
Density	1.1gm/cm3	1.4gm/cm3
Melting Point	200^0C	173^0C
High Temperature Applicability	Yes	No
Brittleness	No	Yes
Abrasion Resistance	Yes	No

ABS has superiority in temperature applicability, abrasion resistant, not brittle, thus, comparatively the material is selected for the project.

However, the printed mechanism from ABS material failed when load dislodged, and gear messing could not transfer the torque and failed. With two unsuccessful models of the mechanism, the other simpler mechanism was considered.

The reasons for failure of the system as observed are as follows:

a. The gear teeth in contact deformed while transferring torque.
b. Plastic or printed gear does not function as metallic gears.
c. The overall weight of the mechanism was higher than estimated i.e. greater than 120 grams.

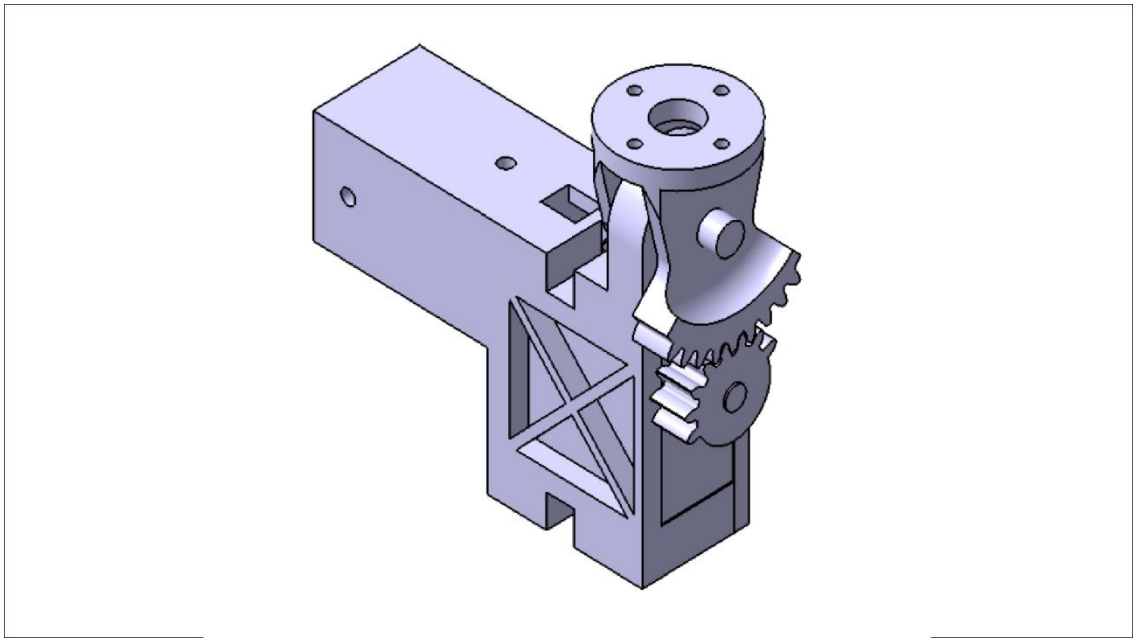

Figure 4.2. 5 Modified Gear Mesh Mechanism with Only Useful Gear Tooth.

If gear mechanism was to be finalized, following points must be considered while designing and fabricating:

a. The gear tooth must be smooth so that it does not abrase from the meshing point.
b. The thickness of the gear must be adequate for proper meshing.
c. It is better to use metallic gears, but this increases the weight of the system and is also difficult to fabricate.
d. Better material must be used to print the gear.

Despite the failure of the system, many things were learned during design and fabrication of the mechanism. It was observed that better design must consist of lesser components and the rotating platform should be closer to the servo's shaft to reduce torque requirement.

4.2.4 Direct Connection of Platform to Servo Shaft

To reduce the number of components, servo was directly connected to the rotating platform in the below shown arrangement. Behind the servo and along its axis, bearing is mounted. A metal shaft is then used to connect the servo housing and the rotating platform. To reduce overall weight a honeycomb structure was used. This design was rejected as the thrust load was transferred to the servo's shaft in radial direction. Also, the moment arm to the servo was not reduced as desired. The used servo could not rotate the platform at optimum speed.

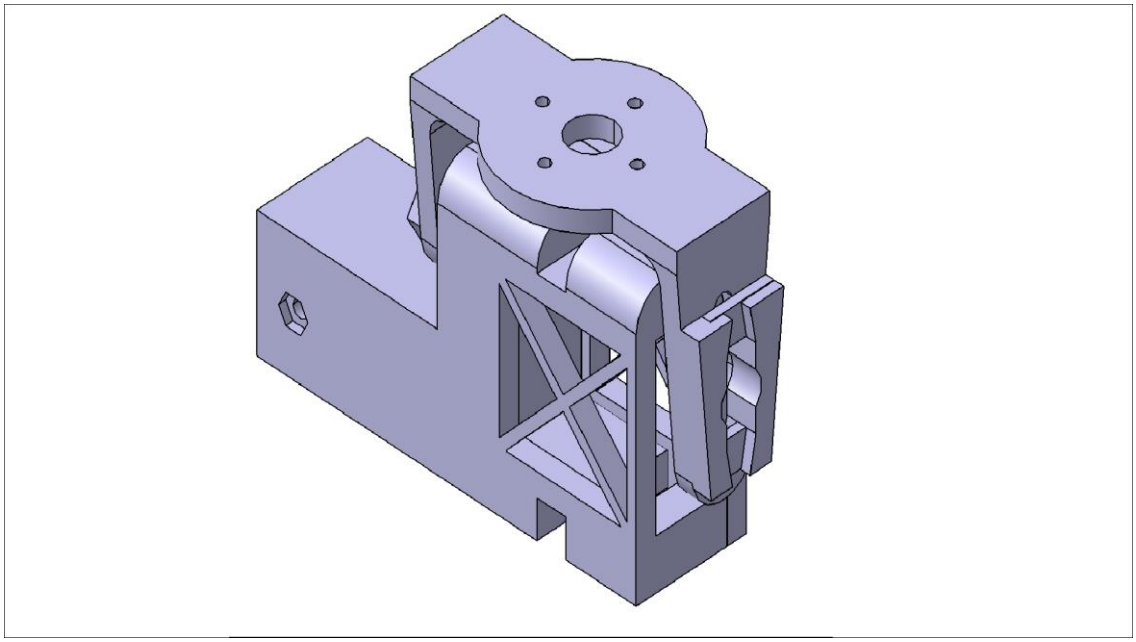

Figure 4.2. 6 Connecting Platform to Attach BLDC Motor Directly to Servo Shaft

4.2.5 Coupling the Platform and the Servo

After the failure of the gear mechanism, coupling system was considered. In this design, servo is directly coupled to the platform via a metal shaft such that servo directly rotates the propulsion system with minimum moment arm. The finite method analysis was performed on this system, and it was observed that the system deformed by only 0.4 mm at 20N thrust on each rotor which is acceptable.

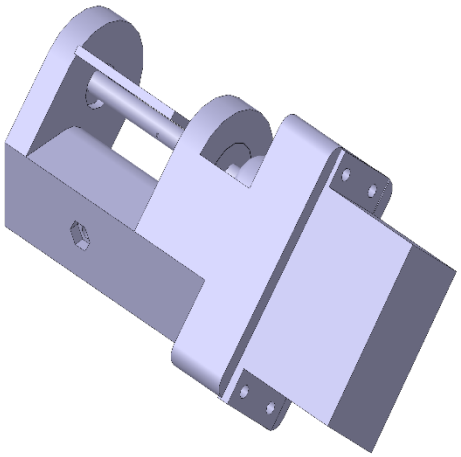

Figure 4.2. 7 Connecting the Servo to the Shaft of Platform Using Coupler

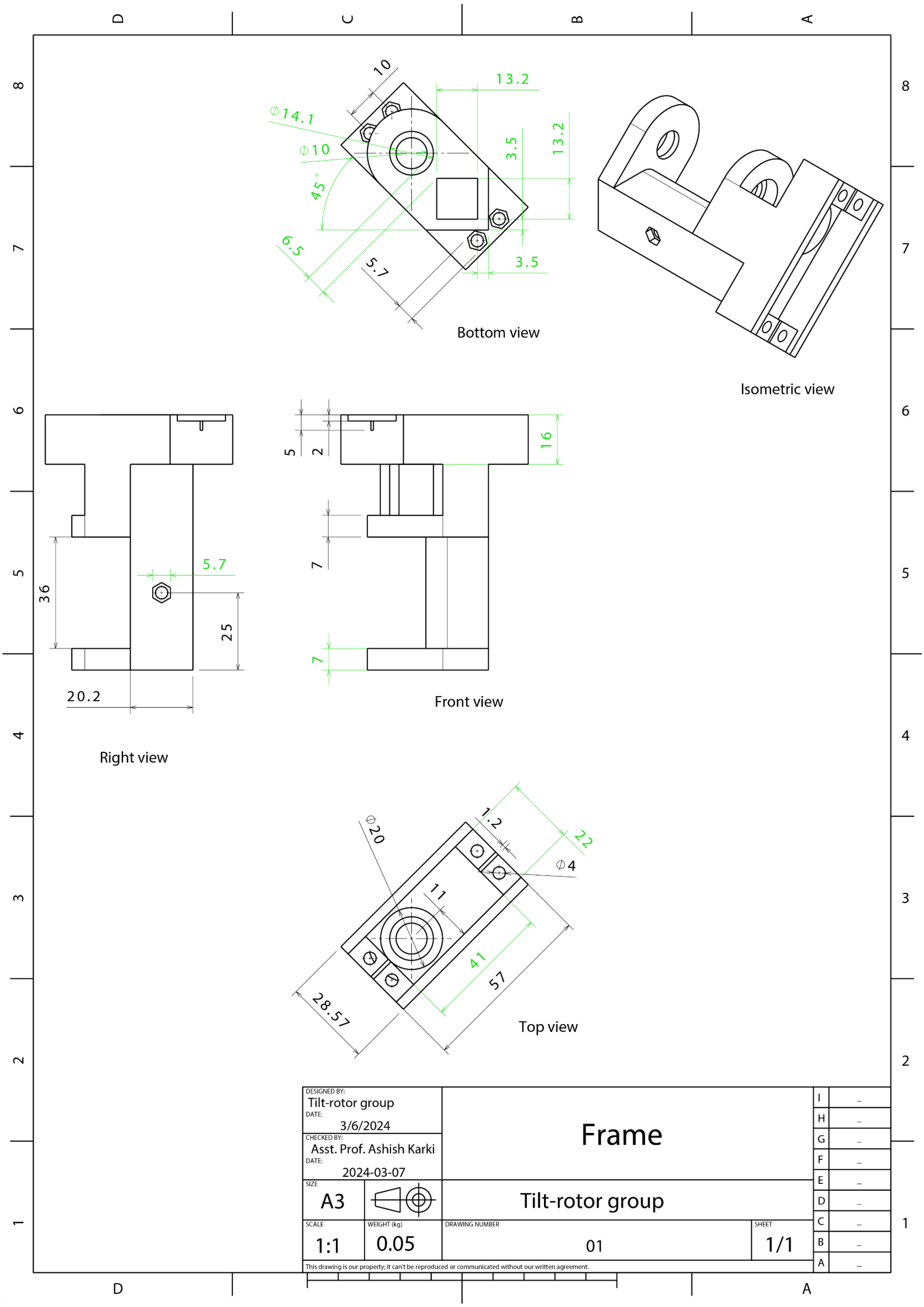

Figure 4.2. 8 Draft of Frame

The major boost in this mechanism is that the moment arm of the system is reduced and the torque from the servomotor is directly transmitted to the platform through the connecting rod. The coupler is also designed, and the printed part also did not fail in the initial phase of the testing.

Along with the iterative design process, material and equipment selection was performed simultaneously. With the available materials and size of the project, different electronics and equipment are selected as they are listed as:

Table 4.2. 2 Equipment List Selected for the Design

Equipment	**Properties**
Motor	
Type	QA2825
Rating	700kv
Mass	170gm
ESC	60A
Control Board	Arduino UNO
Load Cell	
Number	2
Rating	Maximum 10kg of Load
HX11	2
Bearing	Radial ball bearing with internal diameter of 5mm×2
Printing Material	ABS & PLA
Battery	
Rating	11.2 V
Mass	330gm
Energy Density	135 W-h/kg
Servo Motor	MG996R
Modulation	Digital
Torque	6V: 11 kg-cm
Speed	6V: 0.15 sec/60°
Weight	55 g

Dimensions	Lenth: 40.7 mm
	Width: 19.7mm
	Height: 42.9mm
Gear type	Metal
Rotation/Support	Dual Bearings
Pulse Cycle	1ms

4.2.6 Testbench Setup

The test setup has a load cell to measure thrust in zero-to-ninety-degree orientations. The load cell is fixed on horizontal plate. The housing is elevated with a metal tube to avoid propellers striking the ground. The total setup is fixed on a wide wooden base for stability.

The spar of the mechanism is placed and fixed on the housing to measure total thrust of two rotors simultaneously in zero-to-ninety-degree orientations. As the angle of the tiltrotor is changed, the loadcell measures varying thrust in vertical direction.

The varying parameters in this test shall be the speed of rotors and the tilting time of the mechanism.

Using the observations of the test, we aim to realize optimal tilting time and varying rate of rotors' speed required for stable transition from VTOL configuration to fixed wing configuration and vice-versa.

Meanwhile, the servomotor is chosen as MG996R. We decided on this servomotor as it is quite easily accessible providing enough torque required for our tilting mechanism. It is used to tilt the BLDC motor mounted on the plate in the required orientation with sufficient torque.

4.3 Numerical Interpretation of the Mathematical Model

The mathematical model is derived for the generalized representation of the UAV and the tilt-mechanism. The numerical representation of the UAV, and the mechanism and variance of the properties in altitude, attitude and other properties must be checked. The obtained result of the numerical representation of the system can be stated as:

For UAV considered, initially, minimum required thrust to hover the UAV is considered and using the plot, minimum required velocity plot at different angle of transition was calculated as:

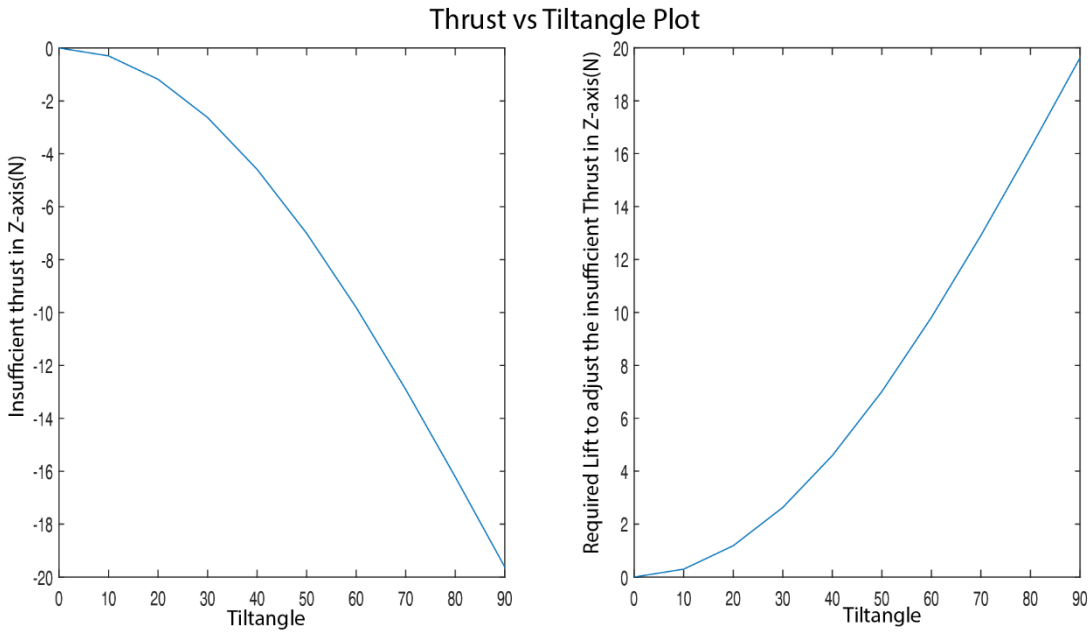

Figure 4.3. 1 Thrust Insufficient in Z-axis to Sustain Weight of UAV versus Tilt-Angle of the Propulsion System.

From the above plot, it was determined the minimum velocity required at each instance to overcome the insufficient lift and plotted to cross related the required velocity versus the tilt angle of the propulsion system. The required velocity plot versus tilt-angle can be represented as:

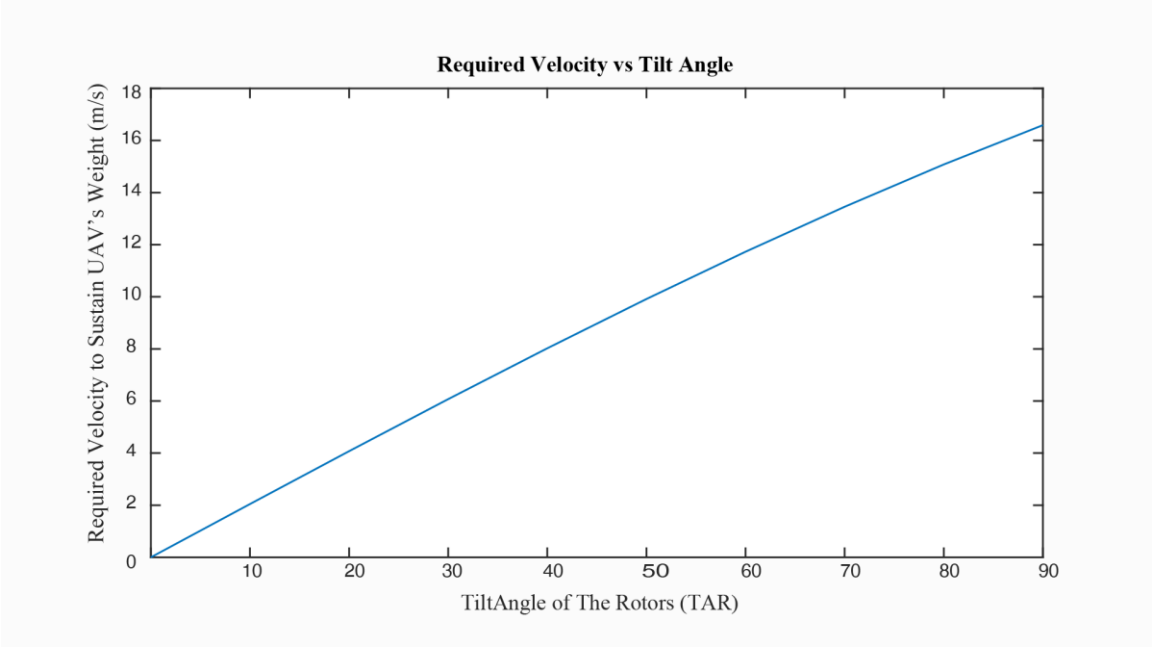

Figure 4.3. 2 Required Velocity to Overcome Insufficient Thrust in Z-axis in Different Angle Plot.

From the above plot, and available thrust from the propulsion system in X-direction of the UAV, available thrust versus the required velocity, a plot was plotted for determining the available thrust for acceleration to reach the required velocity.

During the plotting of the thrust available in X-direction, consideration of the drag produced at each instance due to velocity was considered. This was done to effectively plot the available thrust and determine the time required to accelerate to the velocity required precisely.

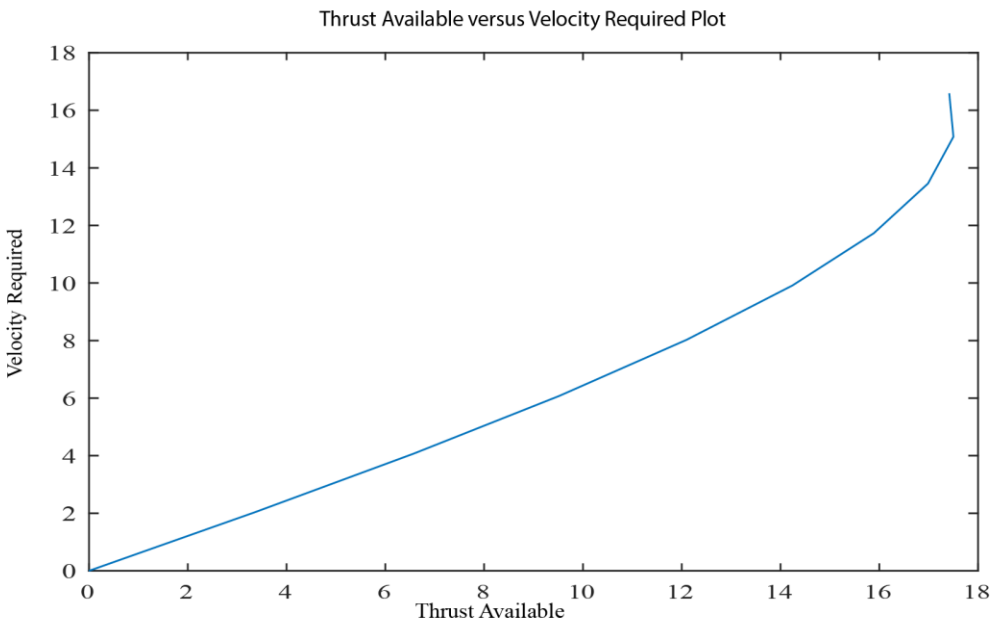

Figure 4.3. 3 Thrust Available at Each Angle of Tilting versus Velocity Required to Provide Insufficient Lift.

From the above two plots, angle at which stall velocity reached was determined as found as it lied in between the range of 40^0 and 50^0. This helped to determine the altitude lost during transition. Moreover, at just hover condition, the transition time is minimum which was determined solving the general equations of motion.

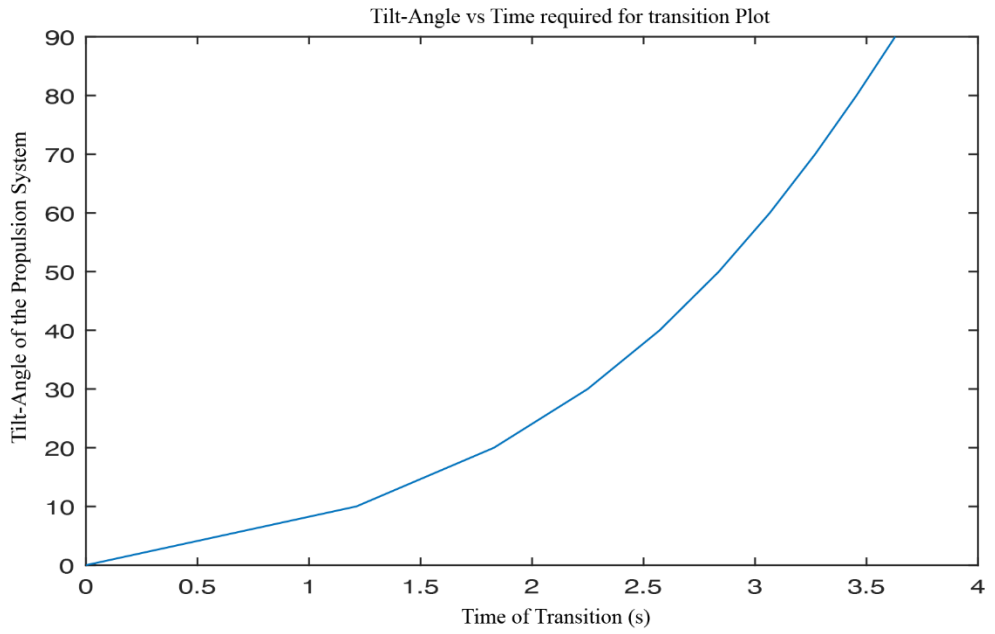

Figure 4.3. 4 Relationship Plot Between Angle of Tilt and Time Required to Transit.

From the plot, the determined maximum amount of time required for transition was 3.7 seconds.

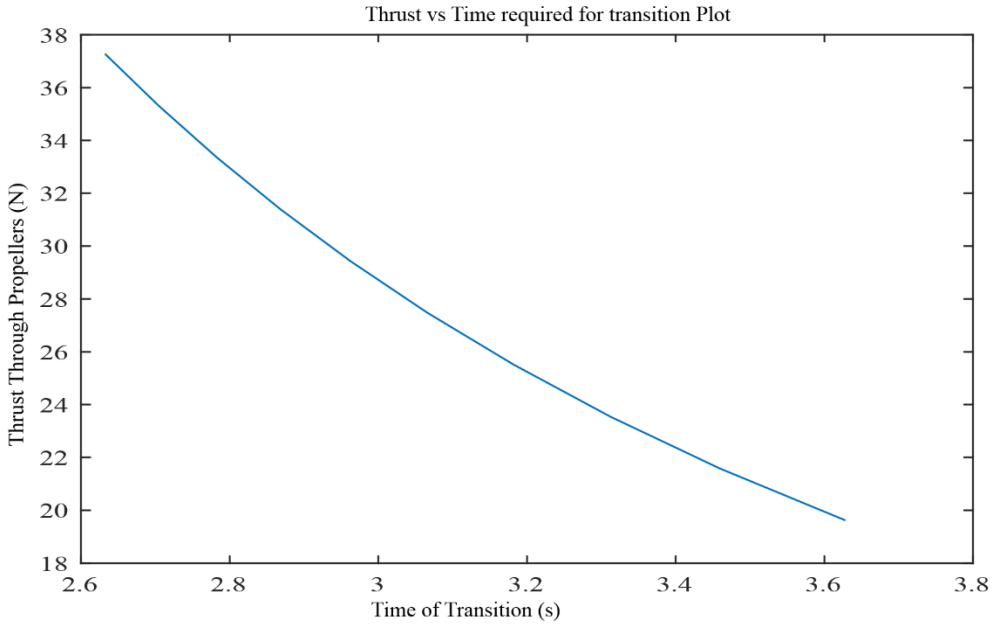

Figure 4.3. 5 Relationship Plot Between Thrust through Propulsion System and Transit time from Vertical to Horizontal Position.

The above plot was generated such that the velocity overcame the loss in vertical thrust and wing provided the sufficient lift to over at the altitude at which stall velocity was achieved.

The velocity at cruise reached at each thrust such that lift generated by the wing sustained the altitude after stall velocity plot can be represented as:

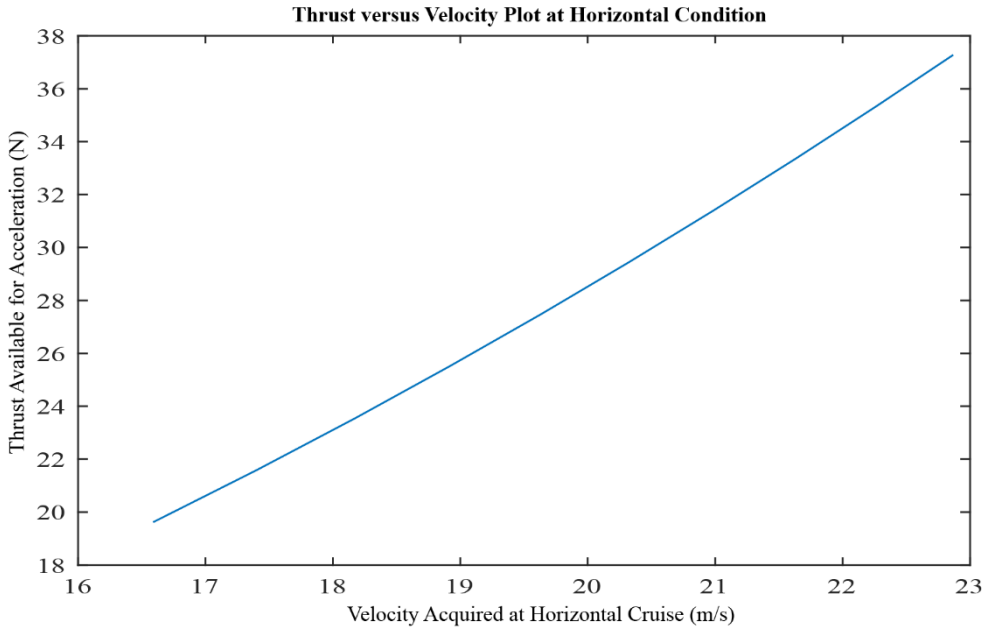

Figure 4.3. 6 Relationship Plot for Available Thrust for Acceleration versus Velocity Acquired at Cruise Condition.

Limiting the cruise velocity to the velocity at minimum condition of hover, and the transition time was determined that pointed out the time required for transition decreased from 2.6 seconds to 1.9 seconds for maximum thrust.

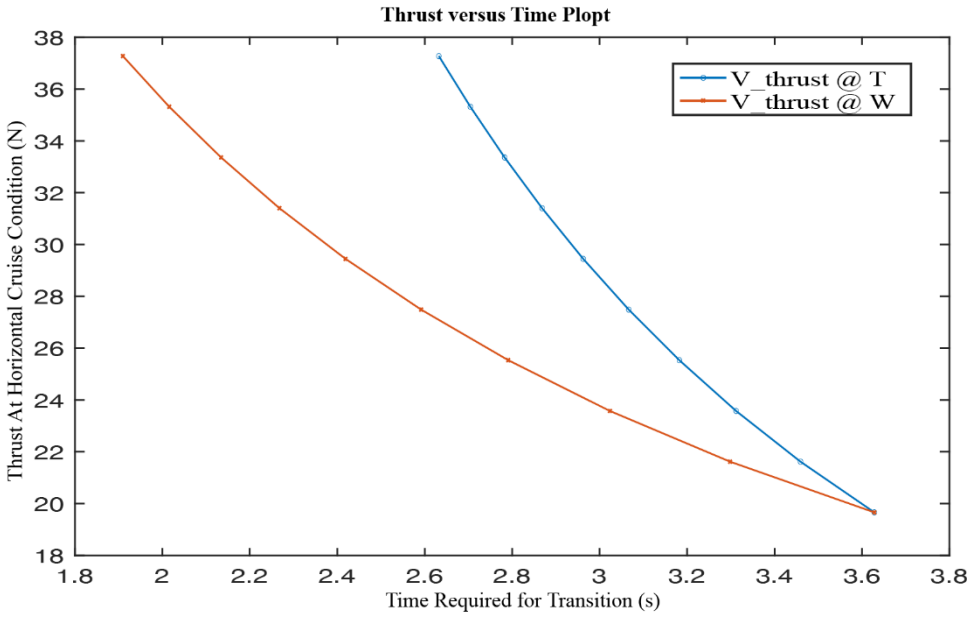

Figure 4.3. 7 Time Required to Complete Tilting at Different Thrust When Cruise Velocity is Fixed and When Cruise Velocity is Thrust Dependent.

Here, V_thrust@T is the plot at which velocity varies with the thrust available and V_thrust@W is the plot at which velocity was kept constant for any thrust available to the velocity at weight balance condition.

As initial conditions of the flight lagged the velocity and no evident lift through the wings till stall velocity, calculating maximum height decay in the flight, till stall velocity for V_thrust@T condition,

Table 4.3. 1 Table Representing Altitude Decay in Variable Thrust from Propulsion System Before Reaching Stall Velocity

Θ	T= 19.62 N	T= 21.5N	T= 23.54 N	T= 25.51 N	T= 27.47 N	T= 29.43 N	T= 31.39 N	T= 33.35 N	T= 35.32 N	T= 37.2N
0^0	0	0	0	0	0	0	0	0	0	0
10^0	0.109	0.328	0.328	0.328	0.328	0.328	0.328	0.328	0.328	0.328
20^0	0.333	0.777	0.777	0.777	0.777	0.777	0.777	0.777	0.777	0.777
30^0	0.678	1.354	1.354	1.355	1.354	1.354	1.354			
40^0	1.152	2.067	2.067	2.068	2.067	2.067	2.067			
50^0	1.764	2.926	2.926							

The consideration of altitude decay is done only till the range of where stall velocity was not reached. From the altitude decay plot, it was observed that despite the change in transition time in different scenario for the tiltrotor, the altitude decay remained somewhat constant and as the thrust for hover condition increased, the stall velocity was reached earlier, and the amount of altitude decay was limited. In this plot, no lift through wings prior to stall velocity was added that could overcome the altitude decay to observe the maximum altitude that could be lost. All the values of altitude lost were in S.I. units.

Furthermore, user defined velocity that could just sustain the weight was evaluated to check the overall altitude decay in different conditions of flight. It was observed that up to 5.4 m altitude could be lost in such conditions when the thrust from motor was

23.54N. The obtained values for different thrust were plotted for cross relation and comparison among each other.

It was also observed that, in each instance of thrust available, the distance travelled when transiting from vertical to horizontal position of propulsion system was same and covered 27.37 m.

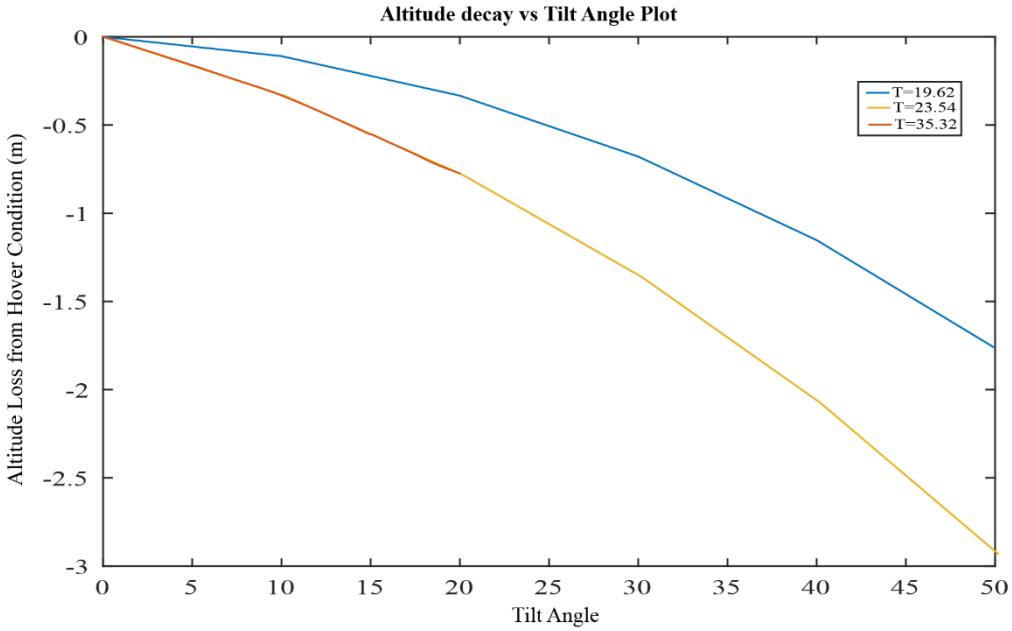

Figure 4.3. 8 Altitude Decay at Different Thrust Available Conditions Before Reaching Stall Velocity.

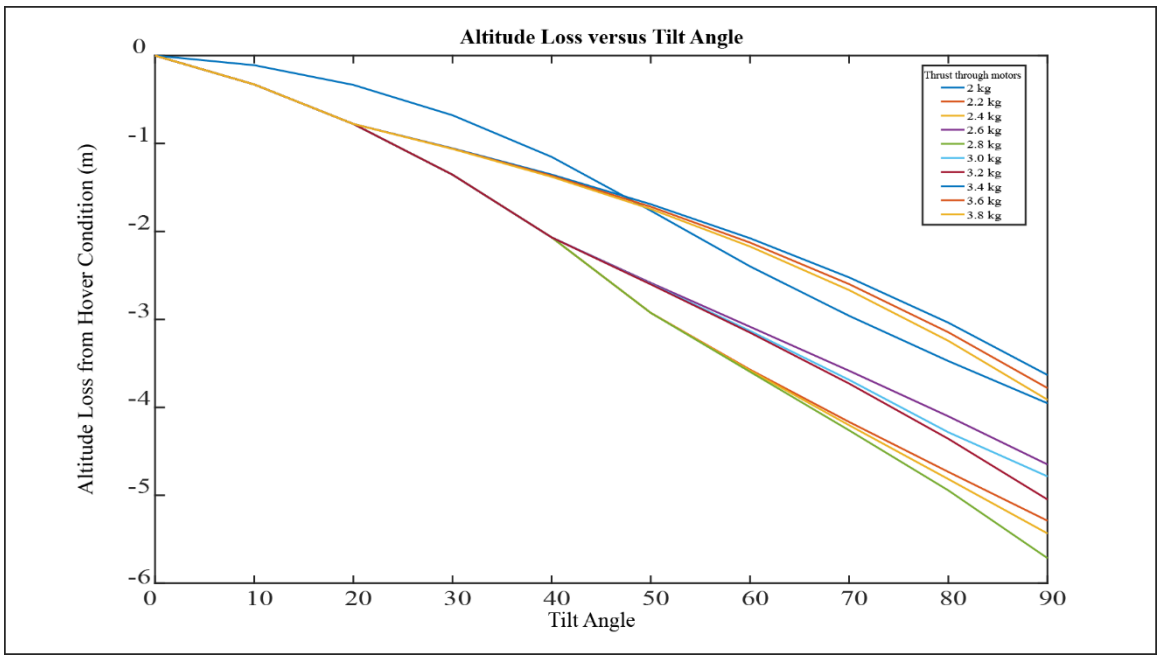

Figure 4.3. 9 Altitude Decay in Variable Thrust from Propulsion System for Fixed Velocity at Cruise Condition.

Meanwhile, when the thrust (ω) was to be increased to sustain the loss of altitude, it was obtained that when stall velocity was reached 45^0, overall, of 18.9% of ω was to be increased with respect to ω at hover condition. In terms of the thrust needed to be increased with respect to thrust at hover condition was 41.4%.

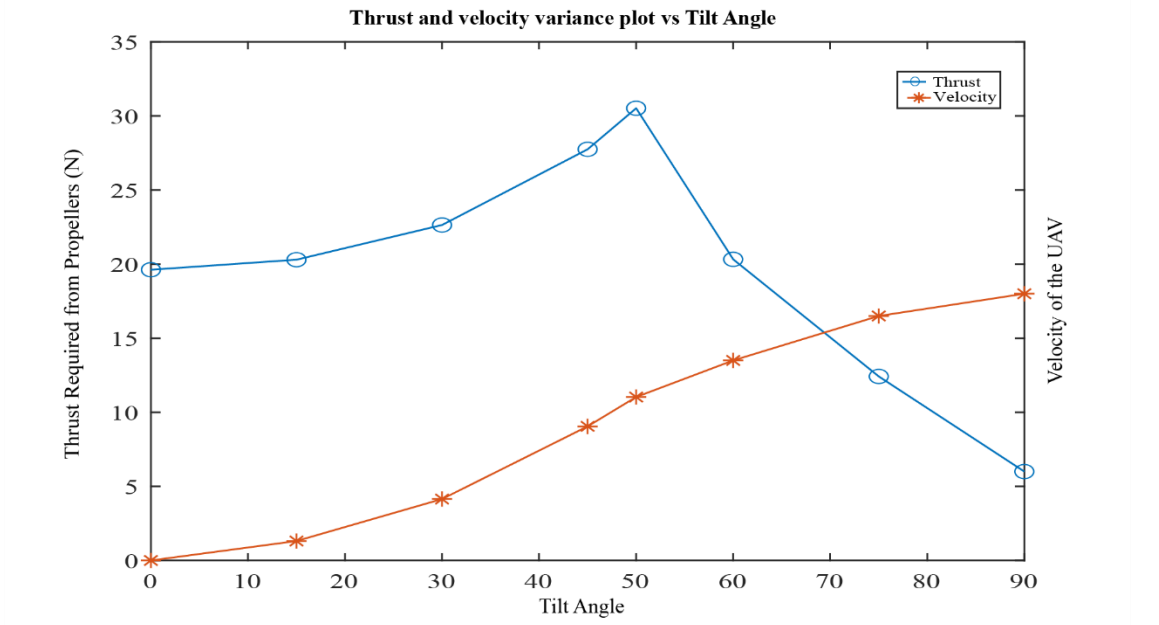

Figure 4.3. 10 Thrust Required versus Angle of Tilt of the Propulsion System to Maintain the Altitude of Hover.

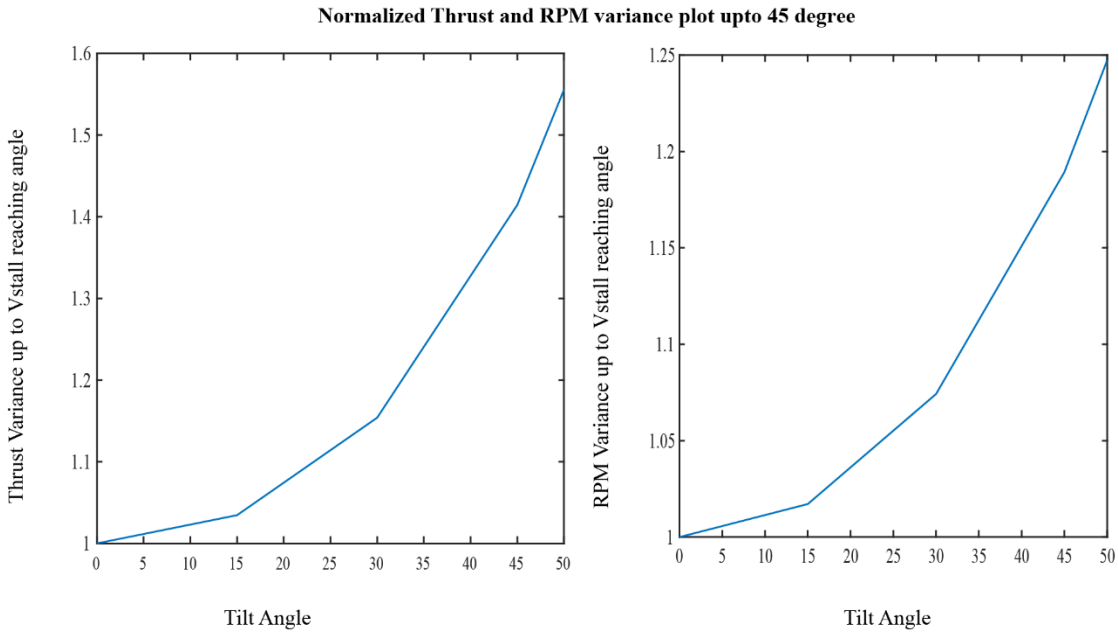

Figure 4.3. 11 Normalized Plot of Thrust and RPM Change versus Angle of Tilt up to Stall Velocity Including Margin of Safety.

From normalized ω plot, it was observed and obtained that between 0^0 and 15^0, 1.7% of initial ω had to be increased, i.e. at 15^0, ω_{15} had to be 1.7% more than ω_0. Similarly, at 30^0, ω_{30} had to be 5.59% more than ω_{15} or 7.47% of ω_0 and at 45^0, ω_{45} had to be 10.68% more than ω_{30} or 18.9% more than ω_0.

The calculations of the omega variance were performed up to 45^0 only because, from previous mathematical plots, it was observed that least that stall velocity was reached was 45^0 of the tilt and with increase in thrust (or ω) at hover condition, stall velocity was reached earlier.

The calculations of the omega variance were performed up to 45^0 only because, from previous mathematical plots, it was observed that least that stall velocity was reached was 45^0 of the tilt and with increase in thrust (or ω) at hover condition, stall velocity was reached earlier.

The thrust requirement and velocity to be obtained from 60^0 to 90^0 was fixed, so that it would be easier for calculations and common cruise velocity could be obtained at every flight after transition.

Table 4.3. 2 Fixed Velocity and Required Thrust for Different Position of Angle of Tilt of Propulsion System to Avoid Altitude Loss.

Angle	Thrust required from propellers (N)	Velocity (m/s)
60^0	20.3	13.5
75^0	12.4	16.5
90^0	6	18

As the time intervals were linearized and distributed evenly for smooth transition and include no extra load to the servo, acceleration would be dependent to the time interval and varied accordingly.

4.4 Experimental Results and Bench Tests

The rigidity of the mechanism hub was tested after attachment to the motors to test whether they would fail in static conditions. In the hub, attached to spar, known weights were hung to check whether they would fail in static structural load test.

The experiment showed positive results and no visible cracks and bending were observed. This showed that the designed hub was statically rigid and could hold the minimum approximated weight.

From the available propellers in the market and in the laboratory, suitable and applicable propellers for the project were chosen and propeller constants were determined.

The obtained propeller constants for the chosen three propellers were,

Table 4.4. 1 Selected Propellers and Experimentally Obtained Propeller Constant.

Propeller	Maximum Thrust obtained (kg)	Voltage Applied	Propeller Constant (k_p) $Ns^2/(rad)^2$
12×50	3.1	22.4 V	1.15×10^{-5}
13×60	3.6	19.2 V	182×10^{-5}
24×45	6.2	22.4 V	2.3×10^{-5}

For the experimental validation of the variance of the ω for keeping the Z-component of the thrust from propulsion system constant, using the tachometer, variance of the ω was checked in between 0^0 to 50^0 and the obtained ω plot was plotted to check with the numerical data. Initially, thrust to throttle from the controller was plotted to obtain the relationship. Also to observe the variance of thrust in Z-direction due to tilting of the rotors were obtained. To keep the thrust constant in Z-axis, throttle was increased to 2.2 kg thrust and plotted.

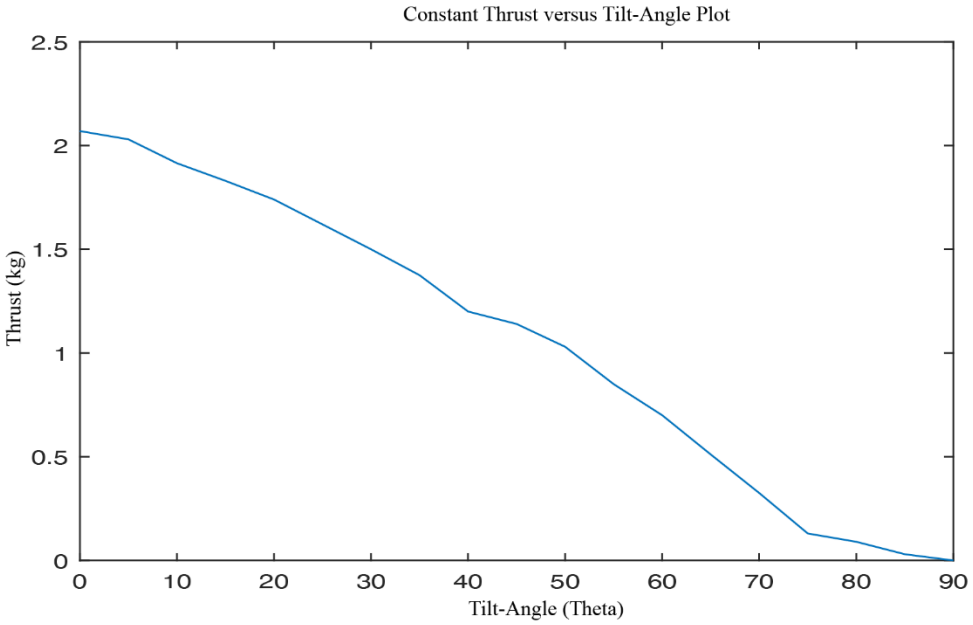

Figure 4.4. 1 Thrust at Different Tilt Angle Plot for 2.1 kg Initial Vertical Thrust

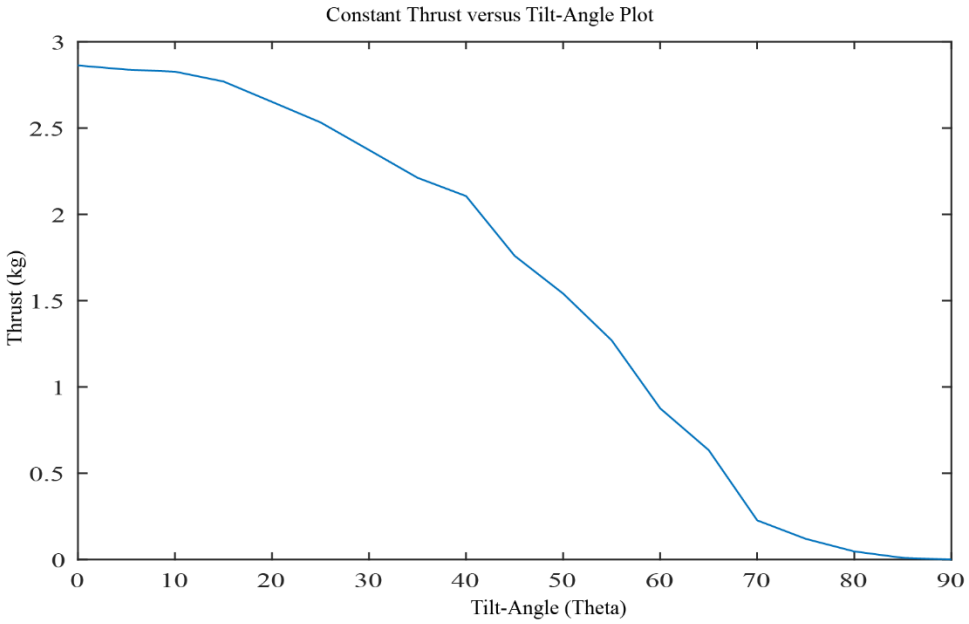

Figure 4.4. 2 Thrust at Different Tilt Angle Plot for 2.8 kg Initial Vertical Thrust.

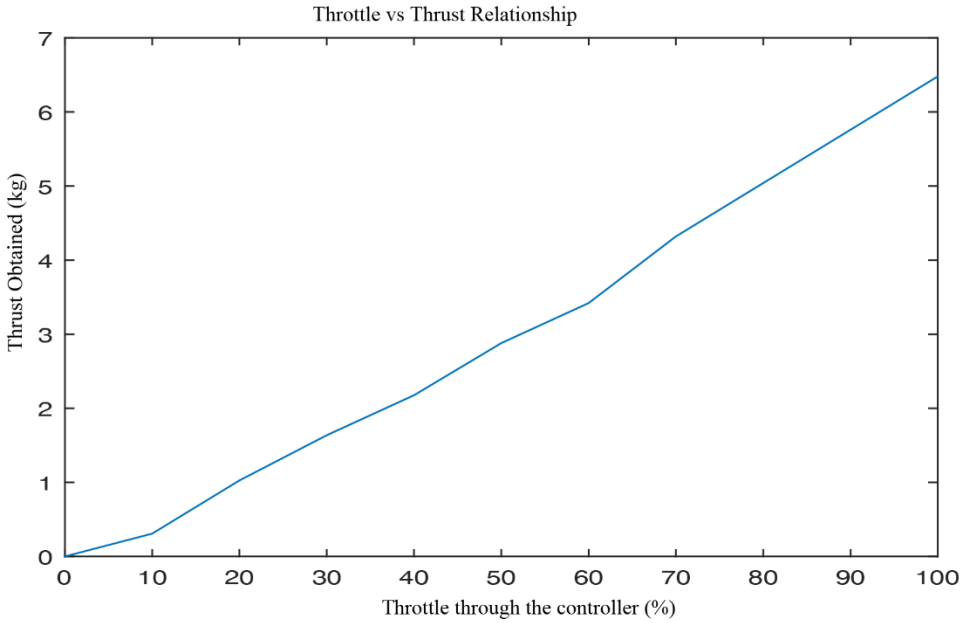

Figure 4.4. 3 Relationship Plot for Throttle from Controller and Variance in Thrust for the System.

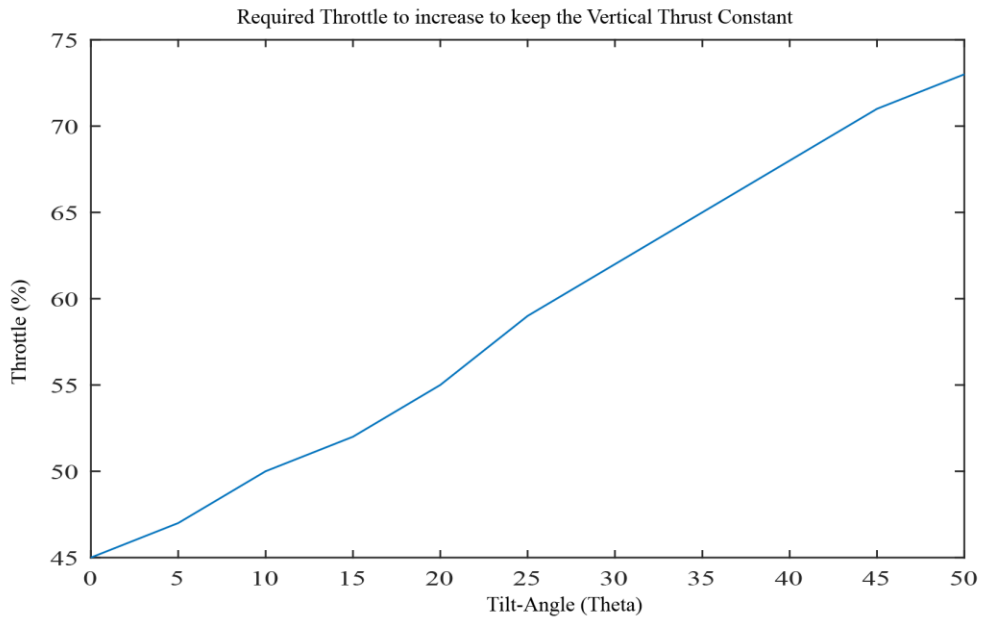

Figure 4.4. 4 Required Throttle to Keep the Vertical Thrust Constant at 2.2 kg Obtained at 45% Throttle.

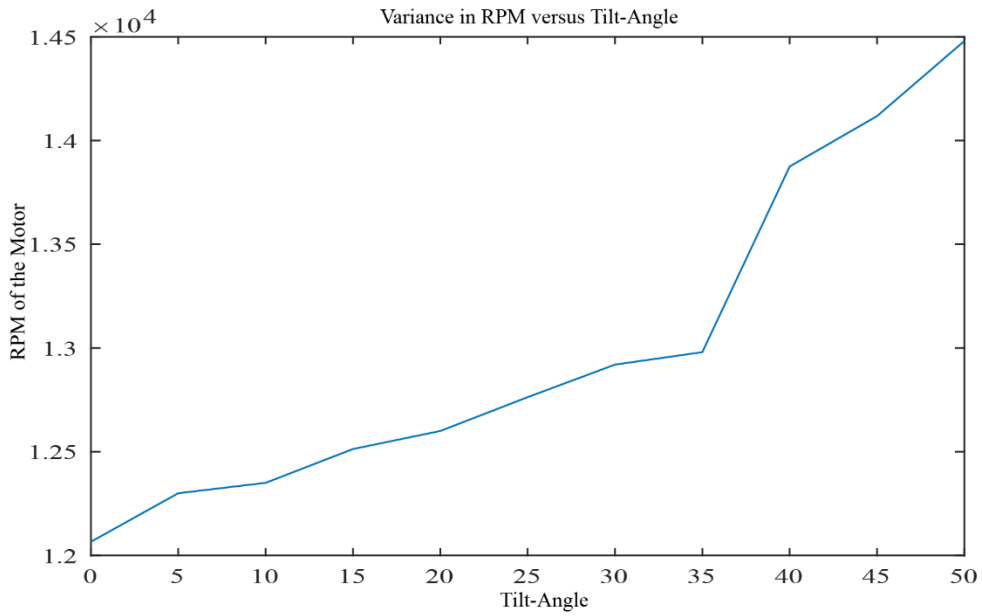

Figure 4.4. 5 Variation of RPM of the Propellers to Adjust Vertical Thrust Constant When Propulsion System Tilts.

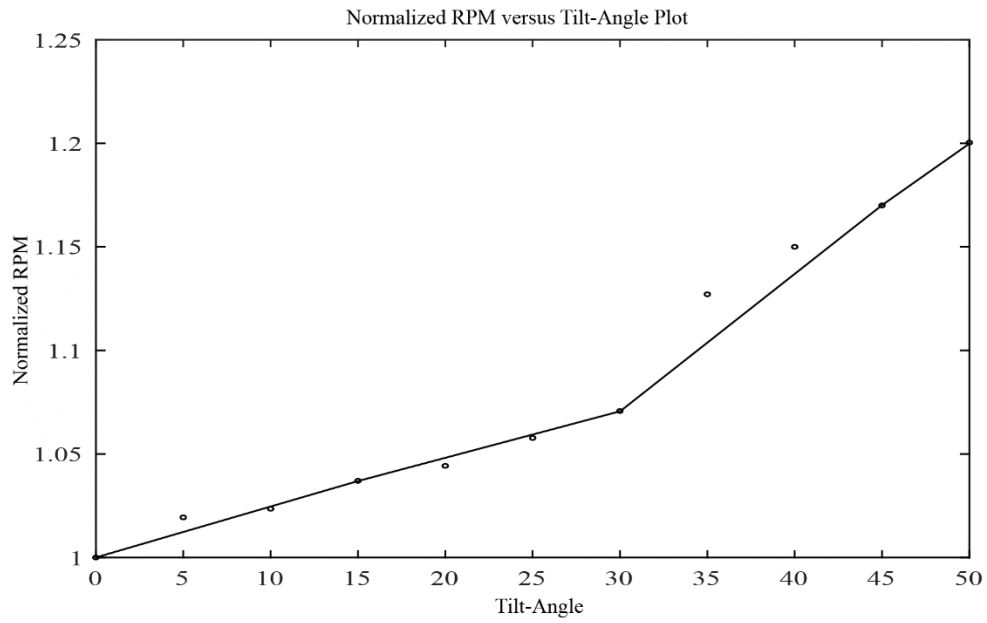

Figure 4.4. 6 Variation of Normalized RPM of the Propellers to Adjust Vertical Thrust Constant When Propulsion System Tilts.

Experimentally, it was observed that the normalized plot of the RPM had 1% error at 30^0 angle tilt and 10% error at 45^0 and 15% error at 50^0. Mathematically, an 18.9% increment with respect to RPM at 0^0 tilt was required, however, only 15% growth was observed. However, the vertical reading of the thrust was constant throughout.

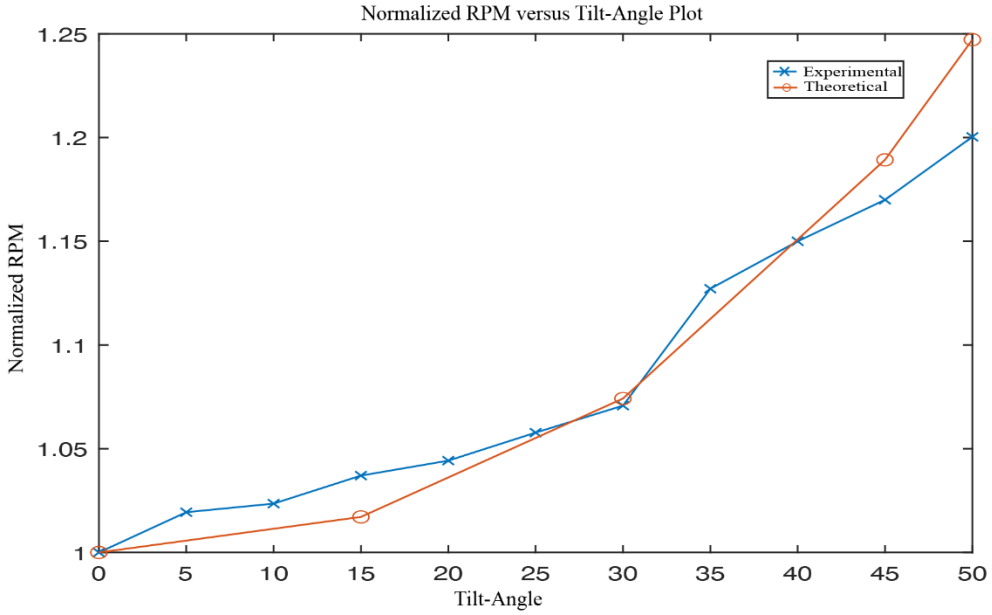

Figure 4.4. 7 Theoretical and Experimental Comparison of Normalized RPM Plot

From the plot, it was found that the rate of change RPM in each interval did not match the theoretical assumption. For the interval of 0^0 to 15^0, the total theoretical percentage that required to change in RPM was 1.7%, however, 3.7% growth was needed to avoid the altitude loss and balance the Z-directional thrust with the propellers. For the interval 15^0 to 30^0, the total growth required theoretically reached the total growth in experiment. The required 7% growth from initial RPM was obtained. For the interval 30^0 to 45^0, the required growth was from 7% to 18.9% however, accounted result showed that the required growth was from 7% to 17% and for 45^0 to 50^0 was from 18.9% to 24% however, the experimental result showed that 20% growth was sufficient to overcome the required thrust loss in Z-direction, up to the point that Lift through the wings were not accounted.

For the experimental observation of the change in RPM of the propellers, a Tachometer was used with an accuracy of 99.9%.

Comparatively, it can be said that the theoretical assumption of the required change in RPM was not required in the experiment. However, the consideration of setup of the experiment must be considered as the ground effect played role. The flow of the air through the experimental setup was not flown through the free airstream, which might have had impact on the experimental result.

For the condition of no altitude loss, it can be stated that the mathematical relation pointed and derived can be applied to use the tiltrotor mechanism in the novel UAV. Also, the thrust required, and velocity required for the UAV to not lose the altitude or gain can be achieved by adjustment of the RPM of the propellers. All the experiments performed for the no altitude loss approach were done with the assumption that the time of transition was linear throughout, and it required 3 seconds to do so.

The experiment was setup to validate whether the mathematical calculations matched up the requirements. And it could be observed that for constant thrust, along with the tilt of the propulsion system, the discrepancy in thrust in Z-direction followed the cosine plot.

However, for the constant thrust, complete experiment could not be performed as it required the development of the UAV and required ideal setup to check the altitude loss. Thus, for the approach of constant thrust, usage, and linkup of the altimeter of the UAV

to calculate the altitude loss and required altitude to be rose for cruise could be performed.

Under the full thrust of the propellers, the physical property change in the motor-servo hub was not observed. The hub was used for handling thrust up to 6.4kg for each and no visible cracks, bending or deformities were observed during inspection. This showed that the mechanism hub designed and fabricated could handle the loads of the propulsion system and could be used and implemented to the VTOL Tiltrotor UAV to be designed. The vibrations through the propellers and no visible impact on the joints, corners and bearing hub of the mechanism hub. The fitted part of the mechanism to the spar had not tightened either, which showed that the load was distributed uniformly.

The results pointed that the mathematical assumption and design of the motor-servo hub could be used and applied for the designing of the VTOL tiltrotor. However, prior to application, it must be modeled as per the UAV to be designed as most of the calculations and experiments of the project were based on the conceptually approximated UAV.

4.5 Limitations and Problems Faced

The limitations of 3D printing material have led to multiple failures in the same mechanism that succeeded in the reference designs. The lack of availability of suitable (13X5.5 as recommended for the motor) propeller in the market led to delay in experimental analysis.

The number of references for the tilt rotor UAV was limited. So, we needed to figure out most of the things on our own including the suitable design and test setup. The flight controller programs are also limited for tilt rotor especially with two rotors configuration.

4.6 Budget Distribution

A budget distribution plan is presented below. This distribution mainly contains hardware and electronic components required for the project. Few of the components were provided by the department as mentioned in the Remarks column.

Table 4.6. 1 Budget Distribution

Particulars	Quantity	Rate (NRs.)	Net Amount (NRs.)	Remarks
Aluminum tube	2	400	800	
Brushless Motor	2	2,000	4,000	Provided by Department
ESC 60A	2	4,200	8,400	Provided by Department
Arduino Uno	2	1,500	3,000	1 Provided by Department
High Torque Servos	2	1,000	2,000	
Electrical And Electronic Components			5,000	
Propeller blade (13X5.0)	1 pair		1,200	Provided by DBF
Propeller blade (10X4.5)	1 pair		180	Provided by Department
Test setup materials			2,500	
Miscellaneous			5,000	
Total			31,980	

CHAPTER 5: CONCLUSION AND FUTURE ENHANCEMENT

This project aimed to design and fabricate a tilt-rotor mechanism for a hybrid Unmanned Aerial Vehicle (UAV) capable of Vertical Take-Off and Landing (VTOL) and fixed-wing operations. The project successfully achieved a functional and efficient tilt-rotor mechanism that could rotate the propulsion system from vertical to horizontal position and vice versa using a servo-actuator and a coupling shaft. A mathematical model of the tilt-rotor mechanism was developed, which could be used for future research and development. A test bench was also created to measure the thrust of the propulsion system in different orientations using a load cell and a flight control board. The project demonstrated the feasibility and potential of the tilt-rotor mechanism for hybrid UAVs.

However, the project faced some limitations and challenges, such as the complexity and uncertainty of the transition phase between VTOL and fixed-wing modes, the lack of a robust control system for the transition, and the limited availability and quality of the materials and components.

For future enhancements, the project suggests the fabrication of a tilt-rotor UAV and the integration of a suitable flight control board with the UAV. The KK2.1 board with Open Aero VTOL firmware is recommended. Conducting a test flight of the UAV is also suggested.

We recommend using time as the deciding factor for transition, with a transition time of approximately 5 seconds. The design of a suitable novel UAV for the installation of the tilt-rotor mechanism is also recommended. For better performance, we highly recommend using a low Reynolds number airfoil, such as the suggested SD7062.

For the variable time approach, we suggest conducting a flight test of the designed UAV to estimate and calculate the altitude drop during the transition phase. This could yield significant results for adopting the transition concept that utilizes available thrust instead of increasing it to maintain altitude.

One of the main problems anticipated during the transition phase was the shifting of the Center of Gravity (CG). To mitigate the CG travel, we recommend using dead weight or a separate mechanism for this sole purpose. It would be much easier to maintain a relatively constant CG position if a motor of a different specification, most probably of lighter weight than the already used QA2825 700 kv motor, is used.

Lastly, we suggest analyzing the airflow over the spar using a smoke generator. This will provide valuable insights into the aerodynamics of the UAV and can help in further optimizing the design.

In conclusion, while the project faced some challenges, it also opened up new avenues for research and development in the field of hybrid UAVs. The tilt-rotor mechanism designed in this project has shown promising results and has the potential to revolutionize the capabilities of future UAVs.

REFERENCES

[1] R. L. Rubin, "Theoretical and Experimental Aerodynamic Thrust Studies of Propellers at Angles of Incidence," University of Canterbury, 2021.

[2] L. Zhong, H. Yuqing, Y. Liying and H. Jianda, "Control techniques of tilt rotor unmanned aerial vehicle systems: A review," *Chinese Journal of Aeronautics,* vol. 30, no. 1, 2016.

[3] N. T. Hegde, V. George, C. G. Nayak and K. Kumar, "Design, dynamic modelling and control of tilt-rotor UAVs: a review," *International Journal of Intelligent Unmanned Systems,* vol. 8, no. 3, 2019.

[4] S. Panigrahi, Y. S. S. Krishna and A. Thondiyath, "Design, analysis, and testing of a hybrid VTOL tilt-rotor UAV for increased endurance.," vol. 21, no. 18, 2021.

[5] J. Tang, K. P. Jain and M. W. Mueller, "QUaRTM: A Quadcopter with Unactuated Rotor Tilting Mechanism capable of faster, more agile, and more efficient flight," *Frontiers in Robotics and AI,* vol. 9, 2022.

[6] Q. ZHANG, J. ZHANG, X. WANG, Y. XU and Z. YU, "Wind Field Disturbance Analysis and Flight Control System Design for a Novel Tilt-Rotor UAV," 2020.

[7] Z. Yu, J. Zhang and X. Wang, "Study of Modeling and Optimal Take-Off Scheme for a Novel Tilt-Rotor UAV," *Sensors,* vol. 22, no. 24, 2022.

[8] Z. Yu, J. Zhang and X. Wang, "Thrust Vectoring Control of a Novel Tilt-Rotor UAV Based on Backstepping Sliding Model Method," *Sensors,* vol. 23, no. 2, 2023.

[9] R. HATORI, S. KONO and K. UCHIYAMA, "Control Strategy for Transition Flight of a Fixed-wing UAV," vol. 12, 2014.

[10] W. H. Song Yanguo, "Design of Flight Control System for a Small Unmanned Tilt Rotor Aircraft," *Chinese Journal of Aeronautics,* vol. 22, 2009.

[11] G. PENNOCK and J. SHIGLEY, THEORY OF MACHINES AND MECHANISMS, McGraw Hill, 2003.

[12] "Arduino," Arduino, 04 january 2024. [Online]. Available: https://www.arduino.cc/. [Accessed 01 October 2023].

[13] D. Trest, "www.dronetrest.com," [Online]. Available: https://www.dronetrest.com/t/kk2-1-flight-controller-guide/379. [Accessed 01 October 2023].

[14] J.-H. Lee, B.-M. Min and E.-T. Kim, "Autopilot Design of Tilt-rotor UAV Using Particle Swarm Optimization Method," in *International Conference on Control, Automation and Systems*, Seol, Korea, 2007.

[15] S. Sharma, R. Sharma, V. Kumar and S. Chandel, "Analysis of a Tiltrotor Vertical Take-off and Landing Unmanned Aerial Vehicle: CFD Approach," in *IOP Conference Series: Materials Science and Engineering*, 2020.

[16] Z. Chen and H. Jia, "Design of Flight Control System for a Novel Tilt-Rotor UAV," *Hindawi,* vol. 2020, no. 2020, p. 14, 2020.

[17] Y. Kang, B.-J. Park, A. Cho, C.-S. Yoo and S.-O. Koo, "Development of Flight Control System and Troubleshooting on Flight Test of a Tilt-Rotor Unmanned Aerial Vehicle," *International Journal of Aeronautical and Space Sciences,* vol. 17, no. 1, pp. 120-131, 2016.

[18] O. Aero, "Open Aero," [Online]. Available: https://openaero.net/. [Accessed 15 January 2024].

APPENDIX

Appendix A: Novel UAV

Appendix Table 1 UAV Parameters.

PARAMETERS	SPECIFICATION
UAV	VTOL, Tiltrotor
Wingspan	124 cm
Wing Cord Length	22 cm
Wing Area	0.267 m^2
Wing Airfoil	Sd7062
Position of C.G. in X axis	6 cm from L.E.
Lift coefficient at 0^0 AOA	0.445

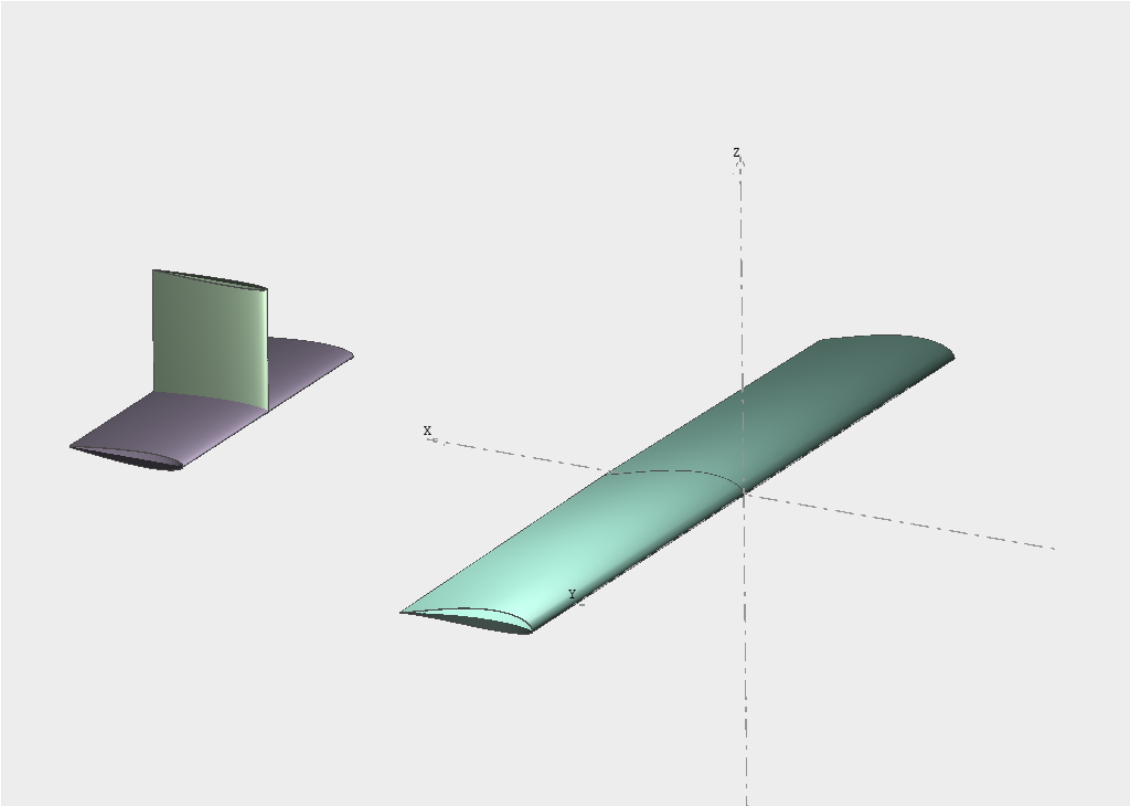

Appendix 1 Novel UAV Designed at XFLR-5

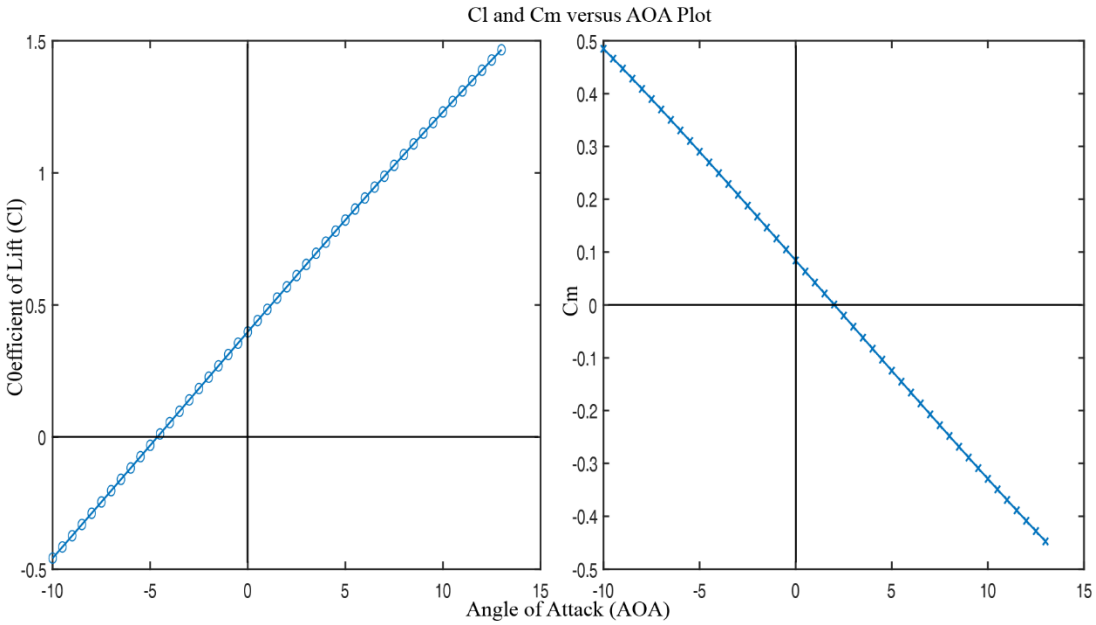

Appendix 2 Cl and Cm Plot Against AOA of the UAV.

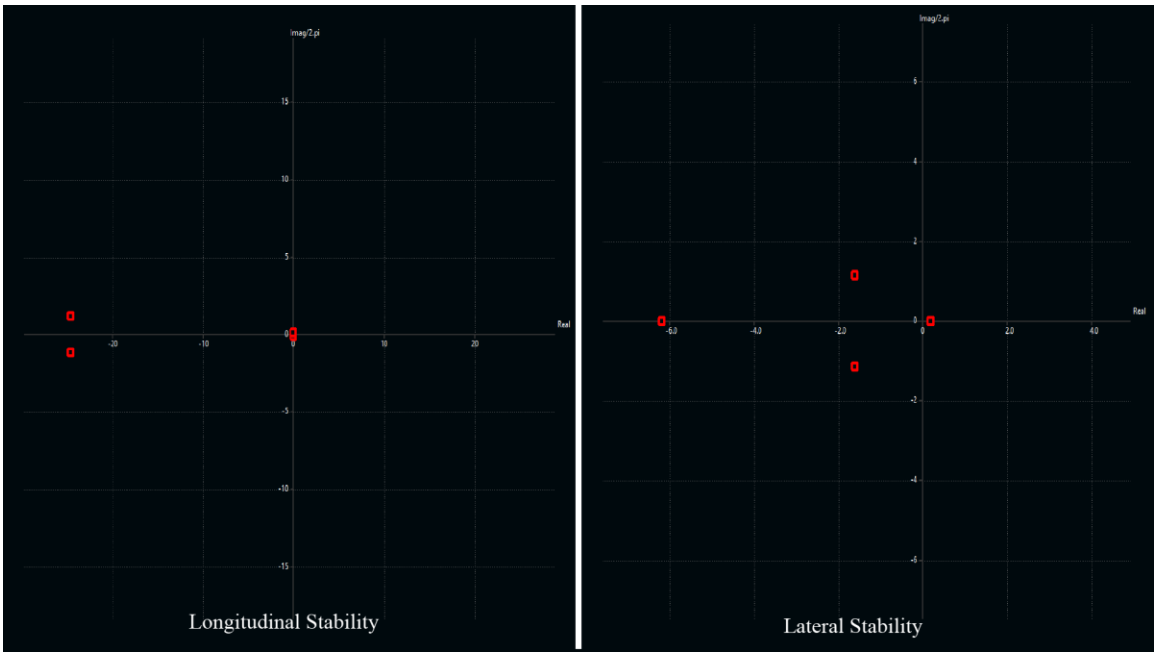

Appendix 3 Static Stability Check of the UAV.

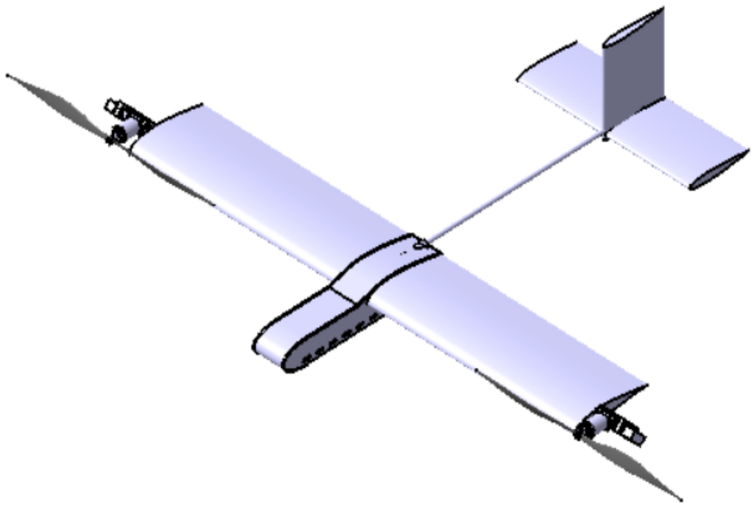

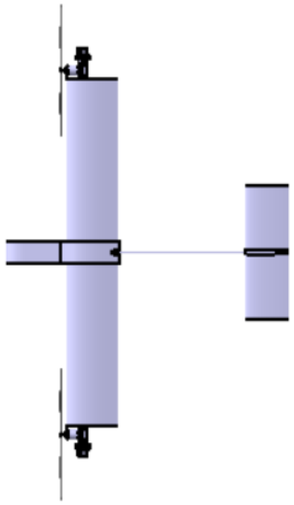

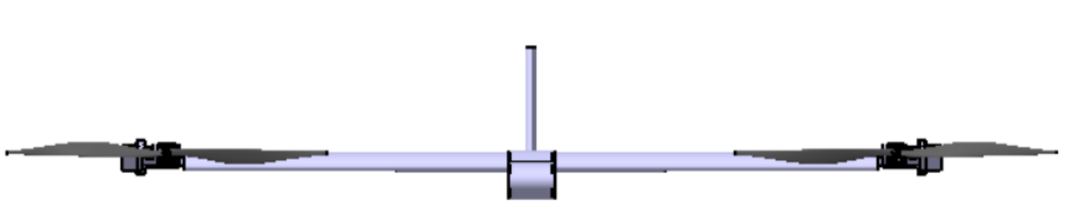

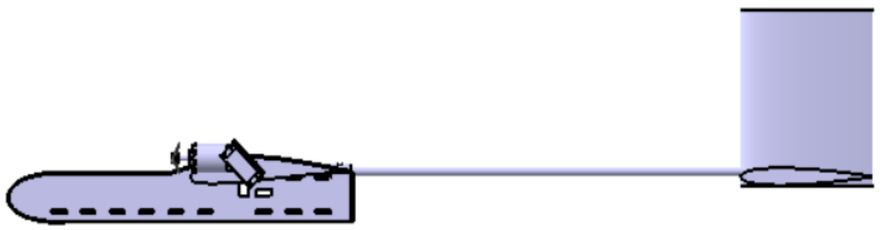

Appendix 4 CAD Model of Novel UAV.

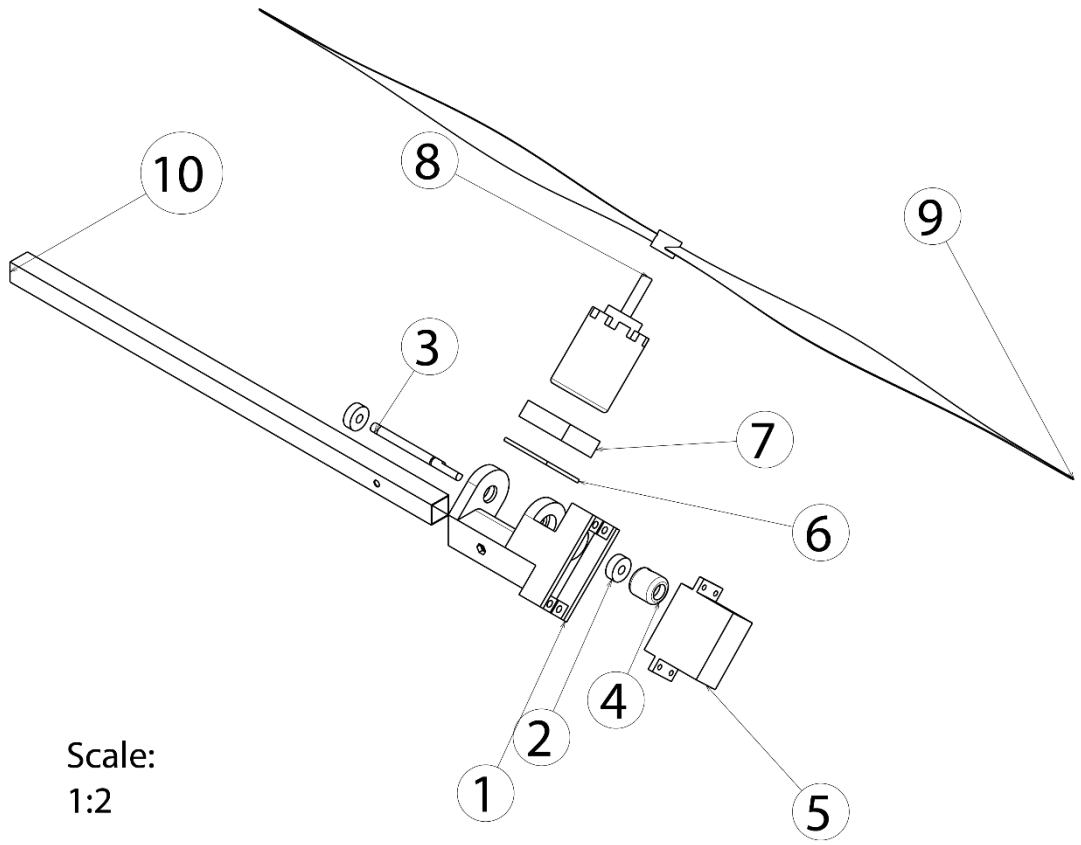

Bill of Material: Assembly of tilt rotor

S.N.	Part Number	Material	Quantity
1	Frame	ABS filament	1
2	Ball bearing 605	Steel	2
3	Shaft	Mild steel	1
4	Servo to shaft coupler	ABS	1
5	Servo MG996R	Metal gear	1
6	Motor mount	Aluminum	1
7	Spacer	Wood	1
8	Motor Qx 2825 700KV	Metal	1
9	Propeller 1350	Plastic	1
10	Spar	Aluminum	1

Appendix 5 Exploded View of the Assembled Mechanism

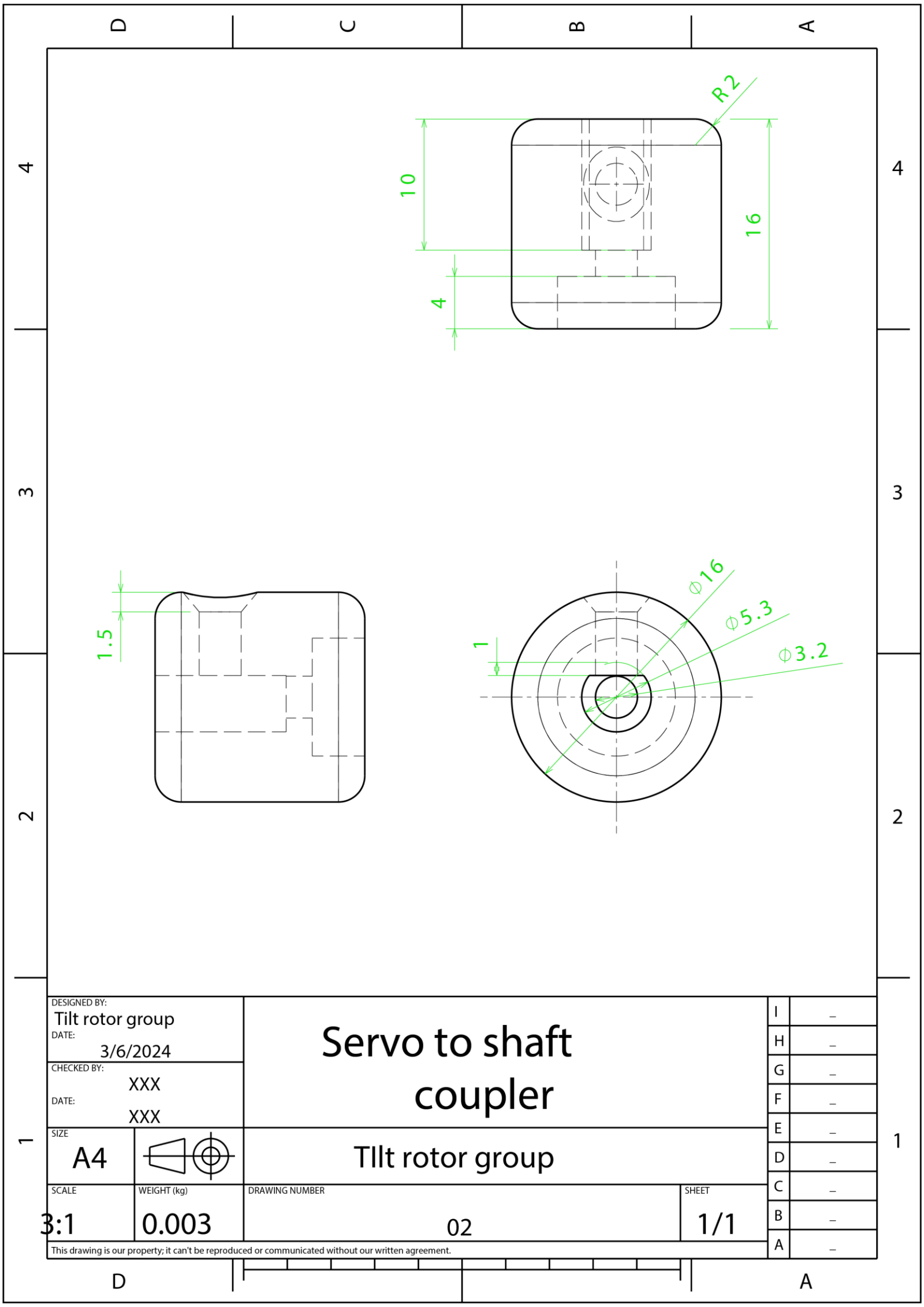

Appendix 6 Draft of Servo Shaft Coupler

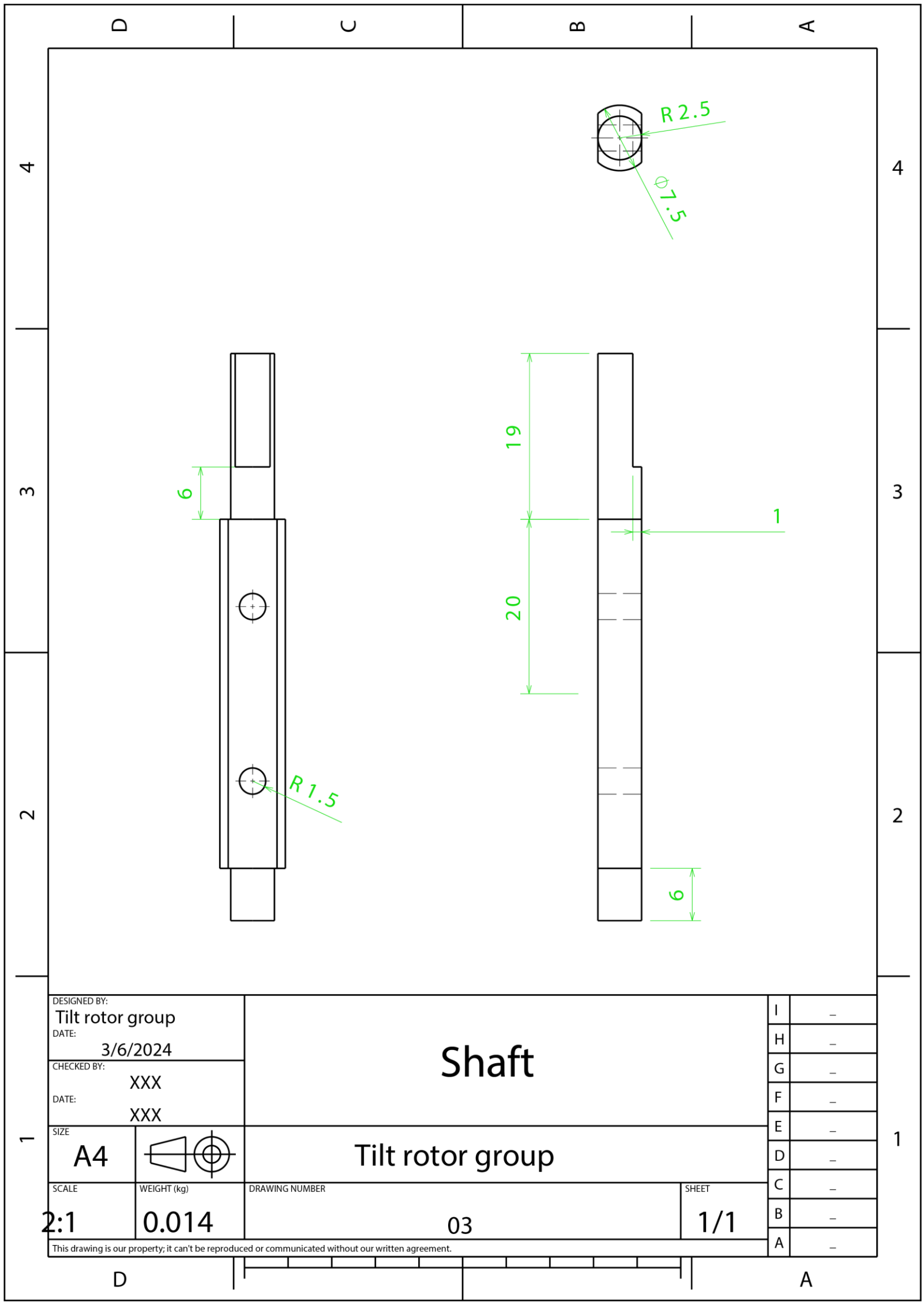

Appendix 7 Draft of Shaft

Appendix B: Mathematical Modeling

Calculations of Thrust and Velocities.

```
%defining initial states for calculations
syms s
xe=0;
ye=0;
ze=0;
phi=0;
theta=0;
psi=0;
Vx=0;%Vxx=linspace(7,27,41);%Vx=18;
Vy=0;
Vz=0;
Vi=(Vx^2+Vz^2)^(1/2);
Vp=0;
Vq=0;
Vr=0;
FR=9.81;
FL=9.81;
g=9.81;
S=0.267;
Cd=0.07;
Cl=0.445;
wB=[0;0;0];
l=1; %length of wing
lz=0; %cg to rotor thrust in z axis
lx=1; %cg ti rotor thrust in x-axis
ly=l/2; %cg to rotor thrust in y-axis
t=linspace(0,3.5,10);

%defining tilt angle
TAR=linspace(0,pi/2,10);
%0 degree
for i = 1:length(TAR)
    TARL = TAR(i);
% Define parameters of the UAV
m=2; %mass of uav in kg
I=[0.014,0,0; 0,0.0004422,0; 0,0,0.114]; %inertia of the uav in kgm^2
rho=1.2; % density of air kg/m3
q=rho*Vi*Vi/2; %dynamic pressure


%define parameters for earth fixed reference
n1=[xe; ye; ze]; %position of the cm of the vehicle wrt inertia
n2=[phi; theta; psi]; % attitude of the cm of the vehicle wrt inertia
nE=[n1; n2]; % overall
```

```
%define parameters for body fixed
V1=[Vx; Vy; Vz]; % linear velocity
V2=[ Vp; Vq; Vr]; % angular velocities
VB=[V1; V2]; %overall

%defining cos and sin values
c1=cos(n2(1)); % c1 is cos phi
c2=cos(n2(2)); % c2 is cos theta
c3=cos(n2(3)); % c3 is cos psi
s1=sin(n2(1)); % s1 is sin phi
s2=sin(n2(2)); % s2 is sin theta
s3=sin(n2(3)); % s3 is sin psi

% DEFINING JACOBIAN MATRIX
J1=[c1*c2, -(s3*c1)+c3*s2*s1, s3*c1*s2;
    s1*c2, c3*c1+s1*s2*s3, -(c3*s1)+s2*s1*c1;
    -s2, c2*s1, c2*c1];
J2=[1/c2, s1*s2/c2, c1*s2/c2;
    0, c1, -s1;
    0, s1/c2, c1/c2];

J=[J1, zeros(3,3);
    zeros(3,3), J2]; %overall J




% defining forces that act
F2=[FR*sin(TARL)+FL*(sin(TARL)); 0; FR*cos(TARL)+FL*cos(TARL)]; % F2 is
Force through thrust, FR is thrust through right, FL is thrust through left
F3=[m*g*s2; -m*g*s1*c2; -m*g*c1*c2]; % F3 is gravity force
F4=[-q*S*Cd; 0; q*S*Cl]; % F4 is drag and lift forces
F1=(F2+F3+F4);
 %store moments
    F1x(i)=F1(1);
     F1y(i)=F1(2);
      F1z(i)=F1(3);

 %Vx=sqrt(-2*F4/(S*Cd*rho));
    %VBdot=F1/2-wB*V1; % xdouble dot finding
    %Lift Drag recording

    %defining moments
   Len=[0,-lz,ly; lz,0,-lx;-ly,lx,0];
% z=Position of motor in z axis from cg
%x= X place displacement in motor during tilt (consideration to be zero for now)
%y= half of wing span or as the motors are placed on wing tip, position of
%motor from cg in y axis
    M2=Len*F2;
```

```
    M3=[0;0;0]; %GYROSCOPIC MOMENT
    M4=[0;0;0]; %AERODYNAMIC MOMENT
    M5=[0;0;0]; %CONTROLSURFACE MOMENT

    M1=M2+M3+M4; %TOTAL EXTERNAL MOMENT

    %store moments
    M1x(i)=M1(1);
     M1y(i)=M1(2);
      M1z(i)=M1(3);

      Lpr=(-1)*F1z;
Vpp=sqrt((2*Lpr)/(rho*S*Cl));
      Zplot=F1z+Lpr;
Vtil=Vpp;
qpr(i)=rho*Vpp(i)*Vpp(i)/2;
%qpr(i)=qpr(1);
Fdrag(i)=-qpr(i)*S*Cd*(Vtil(i)).*(Vtil(i));
%Fdrag(i)=Fdrag(1);z
new = F1x+Fdrag;
new(i)=new(1);
   %for i = 2:length(TAR)
%acc=(Vpp(i)-Vpp(i-1))/t(2);
%acc(i)=acc(1);
%end
%% height decay section
if i> 1
fz_loss=F1z-F1z(i);
end
end
tar=(180/pi)*TAR;

%% generate plot
figure;
plot(tar, F1x);
xlabel('TiltAngle of The Rotors (TAR)');
ylabel('F1x (N)');
title('F1x available at 0m/s velocity vs Tilt Angle');

figure;
plot(tar, Vpp);
xlabel('TiltAngle of The Rotors (TAR)');
ylabel('Required lift');
title('Required Velocity vs Tilt Angle');
```

Appendix C: Servo Control Code

```
#include<Servo.h>

Servo s1;

Servo s2;


int servoPosition1 = 135; //mechanism 0 degree is equivalent to servo 135 degree for servo 1

int servoPosition2 = 60;   //mechanism 0 degree is equivalent to servo 60 degree for servo 2

float a= 135;

float b= 60;


void setup(){

  s1.write(servoPosition1);

  s2.write(servoPosition2);


  s1.attach(6);

  s2.attach(9);

}


void loop(){

  for(int i=0; i<=18; i++){

    s2.write(b);

    s1.write(a);

    a= a-(107/18);

    b= b+(100/18);

    delay(8000);

   }

}
```

Appendix D: Load Cell Calibration

```
#include <HX711_ADC.h>
#if defined(ESP8266)|| defined(ESP32) || defined(AVR)
#include <EEPROM.h>
#endif

//pins:
const int HX711_dout = 4; //mcu > HX711 dout pin
const int HX711_sck = 5; //mcu > HX711 sck pin

//HX711 constructor:
HX711_ADC LoadCell(HX711_dout, HX711_sck);

const int calVal_eepromAdress = 0;
unsigned long t = 0;

void setup() {
  Serial.begin(57600); delay(10);
  Serial.println();
  Serial.println("Starting...");

  LoadCell.begin();
  //LoadCell.setReverseOutput(); //uncomment to turn a negative output value to positive
  unsigned long stabilizingtime = 2000; // preciscion right after power-up can be improved by adding a few seconds of stabilizing time
  boolean _tare = true; //set this to false if you don't want tare to be performed in the next step
  LoadCell.start(stabilizingtime, _tare);
  if (LoadCell.getTareTimeoutFlag() || LoadCell.getSignalTimeoutFlag()) {
```

```
  Serial.println("Timeout, check MCU>HX711 wiring and pin designations");
  while (1);
 }
 else {
  LoadCell.setCalFactor(1.0); // user set calibration value (float), initial value 1.0 may be used for this sketch
  Serial.println("Startup is complete");
 }
 while (!LoadCell.update());
 calibrate(); //start calibration procedure
}

void loop() {
 static boolean newDataReady = 0;
 const int serialPrintInterval = 0; //increase value to slow down serial print activity

 // check for new data/start next conversion:
 if (LoadCell.update()) newDataReady = true;

 // get smoothed value from the dataset:
 if (newDataReady) {
  if (millis() > t + serialPrintInterval) {
   float i = LoadCell.getData();
   Serial.print("Load_cell output val: ");
   Serial.println(i);
   newDataReady = 0;
   t = millis();
  }
 }
```

```
  // receive command from serial terminal
  if (Serial.available() > 0) {
    char inByte = Serial.read();
    if (inByte == 't') LoadCell.tareNoDelay(); //tare
    else if (inByte == 'r') calibrate(); //calibrate
    else if (inByte == 'c') changeSavedCalFactor(); //edit calibration value manually
  }

  // check if last tare operation is complete
  if (LoadCell.getTareStatus() == true) {
    Serial.println("Tare complete");
  }

}

void calibrate() {
  Serial.println("***");
  Serial.println("Start calibration:");
  Serial.println("Place the load cell an a level stable surface.");
  Serial.println("Remove any load applied to the load cell.");
  Serial.println("Send 't' from serial monitor to set the tare offset.");

  boolean _resume = false;
  while (_resume == false) {
    LoadCell.update();
    if (Serial.available() > 0) {
      if (Serial.available() > 0) {
        char inByte = Serial.read();
        if (inByte == 't') LoadCell.tareNoDelay();
```

```
    }
  }
  if (LoadCell.getTareStatus() == true) {
    Serial.println("Tare complete");
    _resume = true;
  }
}

Serial.println("Now, place your known mass on the loadcell.");
Serial.println("Then send the weight of this mass (i.e. 100.0) from serial monitor.");

float known_mass = 0;
_resume = false;
while (_resume == false) {
  LoadCell.update();
  if (Serial.available() > 0) {
    known_mass = Serial.parseFloat();
    if (known_mass != 0) {
      Serial.print("Known mass is: ");
      Serial.println(known_mass);
      _resume = true;
    }
  }
}

  LoadCell.refreshDataSet(); //refresh the dataset to be sure that the known mass is measured correct
  float newCalibrationValue = LoadCell.getNewCalibration(known_mass); //get the new calibration value
```

```
  Serial.print("New calibration value has been set to: ");
  Serial.print(newCalibrationValue);
  Serial.println(", use this as calibration value (calFactor) in your project sketch.");
  Serial.print("Save this value to EEPROM adress ");
  Serial.print(calVal_eepromAdress);
  Serial.println("? y/n");

  _resume = false;
  while (_resume == false) {
    if (Serial.available() > 0) {
      char inByte = Serial.read();
      if (inByte == 'y') {
#if defined(ESP8266)|| defined(ESP32)
        EEPROM.begin(512);
#endif
        EEPROM.put(calVal_eepromAdress, newCalibrationValue);
#if defined(ESP8266)|| defined(ESP32)
        EEPROM.commit();
#endif
        EEPROM.get(calVal_eepromAdress, newCalibrationValue);
        Serial.print("Value ");
        Serial.print(newCalibrationValue);
        Serial.print(" saved to EEPROM address: ");
        Serial.println(calVal_eepromAdress);
        _resume = true;

      }
      else if (inByte == 'n') {
        Serial.println("Value not saved to EEPROM");
```

```
      _resume = true;
     }
    }
  }

  Serial.println("End calibration");
  Serial.println("***");
  Serial.println("To re-calibrate, send 'r' from serial monitor.");
  Serial.println("For manual edit of the calibration value, send 'c' from serial monitor.");
  Serial.println("***");
}

void changeSavedCalFactor() {
  float oldCalibrationValue = LoadCell.getCalFactor();
  boolean _resume = false;
  Serial.println("***");
  Serial.print("Current value is: ");
  Serial.println(oldCalibrationValue);
  Serial.println("Now, send the new value from serial monitor, i.e. 696.0");
  float newCalibrationValue;
  while (_resume == false) {
    if (Serial.available() > 0) {
      newCalibrationValue = Serial.parseFloat();
      if (newCalibrationValue != 0) {
        Serial.print("New calibration value is: ");
        Serial.println(newCalibrationValue);
        LoadCell.setCalFactor(newCalibrationValue);
        _resume = true;
      }
```

```
    }
  }
  _resume = false;
  Serial.print("Save this value to EEPROM adress ");
  Serial.print(calVal_eepromAdress);
  Serial.println("? y/n");
  while (_resume == false) {
    if (Serial.available() > 0) {
      char inByte = Serial.read();
      if (inByte == 'y') {
#if defined(ESP8266)|| defined(ESP32)
        EEPROM.begin(512);
#endif
        EEPROM.put(calVal_eepromAdress, newCalibrationValue);
#if defined(ESP8266)|| defined(ESP32)
        EEPROM.commit();
#endif
        EEPROM.get(calVal_eepromAdress, newCalibrationValue);
        Serial.print("Value ");
        Serial.print(newCalibrationValue);
        Serial.print(" saved to EEPROM address: ");
        Serial.println(calVal_eepromAdress);
        _resume = true;
      }
      else if (inByte == 'n') {
        Serial.println("Value not saved to EEPROM");
        _resume = true;
      }
    }
```

```
  }
  Serial.println("End change calibration value");
  Serial.println("***");
}
```

Appendix E: Load Cell Data Reading

```
#include <HX711_ADC.h>
#if defined(ESP8266)|| defined(ESP32) || defined(AVR)
#include <EEPROM.h>
#endif

//pins:
const int HX711_dout = 4; //mcu > HX711 dout pin
const int HX711_sck = 5; //mcu > HX711 sck pin

//HX711 constructor:
HX711_ADC LoadCell(HX711_dout, HX711_sck);

const int calVal_eepromAdress = 0;
unsigned long t = 0;

void setup() {
  Serial.begin(57600); delay(10);
  Serial.println();
  Serial.println("Starting...");

  LoadCell.begin();
  //LoadCell.setReverseOutput(); //uncomment to turn a negative output value to positive
  float calibrationValue; // calibration value (see example file "Calibration.ino")
  calibrationValue = 696.0; // uncomment this if you want to set the calibration value in the sketch
#if defined(ESP8266)|| defined(ESP32)
  //EEPROM.begin(512); // uncomment this if you use ESP8266/ESP32 and want to fetch the calibration value from eeprom
```

```
#endif
  EEPROM.get(calVal_eepromAdress, calibrationValue); // uncomment this if you want to fetch the calibration value from eeprom

  unsigned long stabilizingtime = 2000; // preciscion right after power-up can be improved by adding a few seconds of stabilizing time
  boolean _tare = true; //set this to false if you don't want tare to be performed in the next step
  LoadCell.start(stabilizingtime, _tare);
  if (LoadCell.getTareTimeoutFlag()) {
    Serial.println("Timeout, check MCU>HX711 wiring and pin designations");
    while (1);
  }
  else {
    LoadCell.setCalFactor(calibrationValue); // set calibration value (float)
    Serial.println("Startup is complete");
  }
}

void loop() {
  static boolean newDataReady = 0;
  const int serialPrintInterval = 0; //increase value to slow down serial print activity

  // check for new data/start next conversion:
  if (LoadCell.update()) newDataReady = true;

  // get smoothed value from the dataset:
  if (newDataReady) {
    if (millis() > t + serialPrintInterval) {
      float i = LoadCell.getData();
```

```
      Serial.print("Load_cell output val: ");
      Serial.println(i);
      newDataReady = 0;
      t = millis();
    }
  }

  // receive command from serial terminal, send 't' to initiate tare operation:
  if (Serial.available() > 0) {
    char inByte = Serial.read();
    if (inByte == 't') LoadCell.tareNoDelay();
  }

  // check if last tare operation is complete:
  if (LoadCell.getTareStatus() == true) {
    Serial.println("Tare complete");
  }

}
```

Appendix F: Experimental Captures

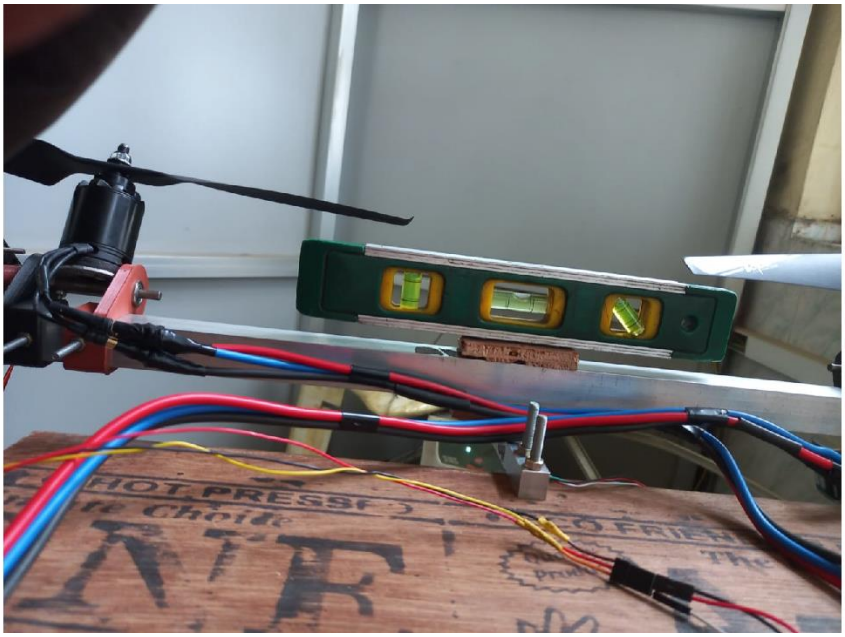

Appendix 8 Leveling of Setup for Data Reading.

Appendix 9 Leveling of Pulley for Loadcell Calibration.

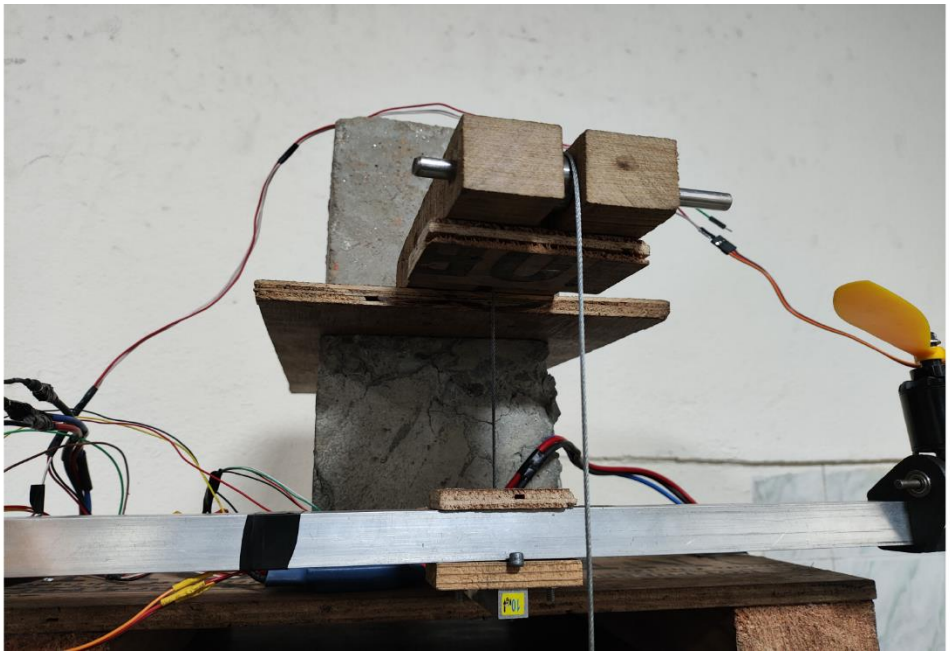

Appendix 10 Pulley System used for Loadcell Calibration.

Appendix 11 Loadcell Calibration Setup.

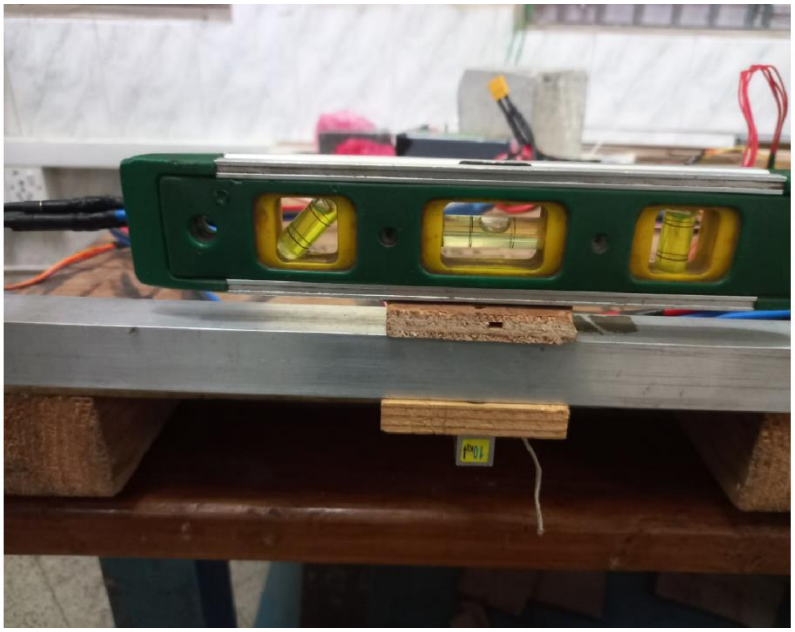

Appendix 12 Leveling of Setup prior to Data Collection.

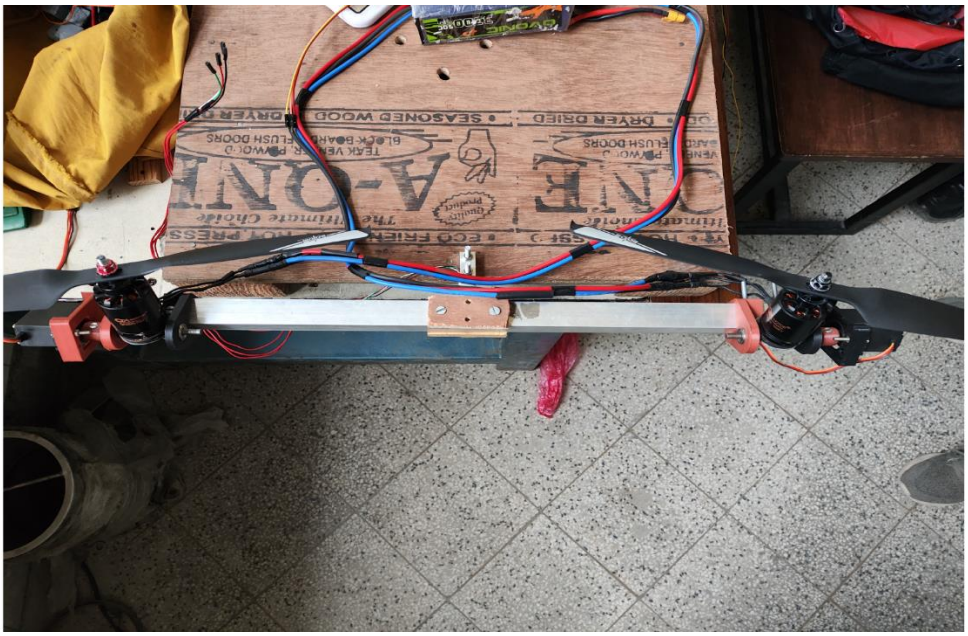

Appendix 13 Complete Experimental Setup for Thrust Calculation at Different Tilt Angles.

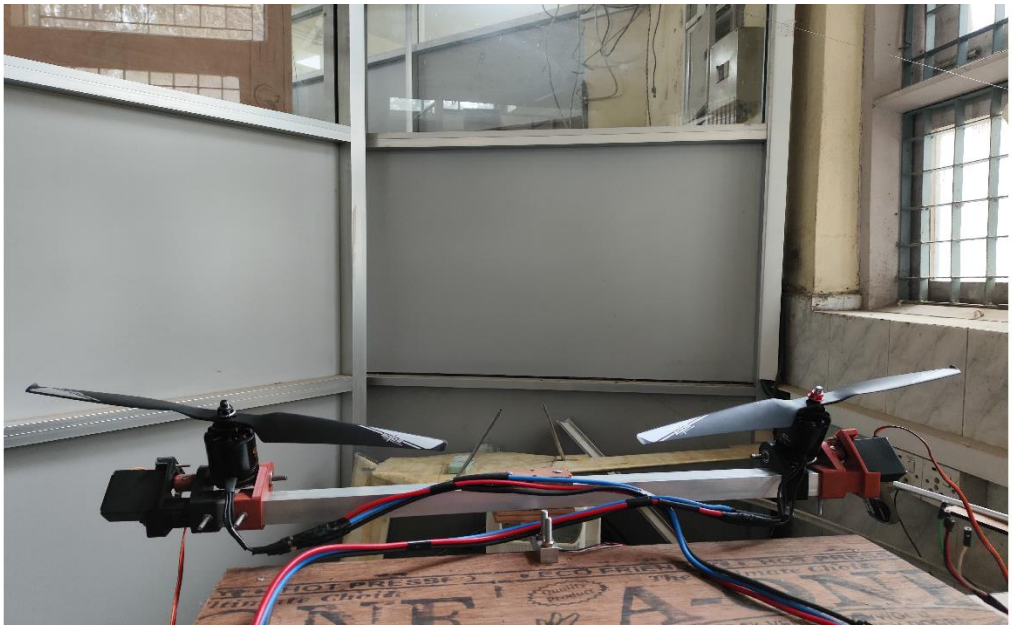

Appendix 14 Setup at a Tilt Angle.

Appendix 15 Motors Orientation Check in Opposite Direction for Moment Generation.

Appendix 16 Leveling of Setup Before Deflection Check of the Setup.

Appendix 17 Tachometer Setup for RPM Calculation for Experiments.

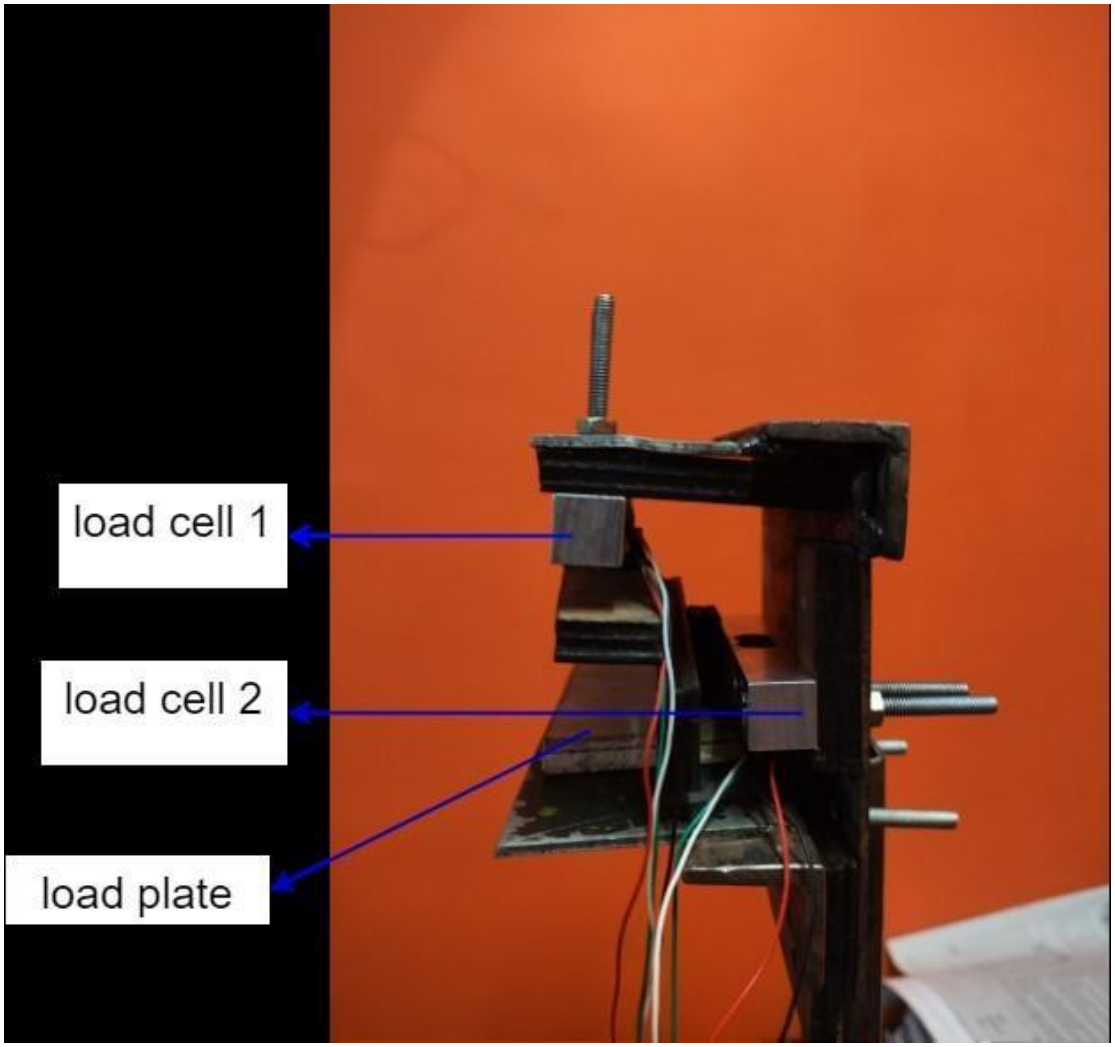

Appendix 18 Dual Load Cell Setup of Test Bench.